Behavioral and genomic sensory adaptations underlying the pest activity of *Drosophila suzukii*

Sylvia M. Durkin[1, 2], Mahul Chakraborty[3], Antoine Abrieux[4], Kyle M. Lewald[4], Alice Gadau[1], Nicolas Svetec[1], Junhui Peng[1], Miriam Kopyto[1], Christopher B. Langer[1], Joanna C. Chiu[4], J.J. Emerson[3], Li Zhao[1*]

1. Laboratory of Evolutionary Genetics and Genomics, The Rockefeller University, New York, NY 10065, USA

2. Department of Integrative Biology & Museum of Vertebrate Zoology, University of California, Berkeley, Berkeley, CA, USA

3. Department of Ecology and Evolutionary Biology, University of California, Irvine, CA, USA

4. Department of Entomology and Nematology, College of Agricultural and Environmental Sciences, University of California, Davis, CA, USA

*Correspondence to: lzhao@rockefeller.edu

ABSTRACT

Studying how novel phenotypes originate and evolve is fundamental to the field of evolutionary biology as it allows us to understand how organismal diversity is generated and maintained. However, determining the basis of novel phenotypes is challenging as it involves orchestrated changes at multiple biological levels. Here, we aim to overcome this challenge by using a comparative species framework combining behavioral, gene expression, and genomic analyses to understand the evolutionary novel egg-laying substrate-choice behavior of the invasive pest species *Drosophila suzukii*. First, we used egg-laying behavioral assays to understand the evolution of ripe fruit oviposition preference in *D. suzukii* as compared to closely related species *D. subpulchrella* and *D. biarmipes*, as well as *D. melanogaster*. We show that *D. subpulchrella* and *D. biarmipes* lay eggs on both ripe and rotten fruits, suggesting that the transition to ripe fruit preference was gradual. Secondly, using two-choice oviposition assays, we studied how *D. suzukii, D. subpulchrella, D. biarmipes* and *D. melanogaster* differentially process key sensory cues distinguishing ripe from rotten fruit during egg-laying. We found that *D. suzukii*'s preference for ripe fruit is in part mediated through a species-specific preference for stiff substrates. Lastly, we sequenced and annotated a high-quality genome for *D. subpulchrella.*

Using comparative genomic approaches, we identified candidate genes involved in *D. suzukii*'s ability to seek out and target ripe fruits. Our results provide detail to the stepwise evolution of pest activity in *D. suzukii*, indicating important cues used by this species when finding a host, and the molecular mechanisms potentially underlying their adaptation to a new ecological niche.

INTRODUCTION

Novel phenotypes can give species the opportunity to occupy a new ecological niche (Mayr, 1960; Moczek, 2008; Muller and Wagner, 1991). Understanding how and when these phenotypes arise is an exciting question in evolutionary biology. Adaptive traits can present as changes to an organism's behavior, physiology, or morphology, and arise through a variety of different molecular mechanisms. In the context of pest species, adaptation to a new ecological niche can come with damaging environmental, agricultural, and economic consequences. Understanding the basis of novel pest behavior can also shed light on the ecological impact of invasive species. Unlike the majority of *Drosophila* flies, the species *Drosophila suzukii* prefers to lay its eggs in ripe as opposed to rotten fruit, causing substantial crop damage and leading to economic losses in the fruit industry (Rota-Stabelli et al., 2013). Although originally categorized in Japan and likely to be native to East Asia, within the past decade *D. suzukii* has spread throughout Europe and North America (Adrion et al., 2014; Fraimout et al., 2017; Paris et al., 2020). Preference for ripe fruit is thought to have evolved along the lineage leading to *D. suzukii*, as *D. melanogaster* and other outgroup species, including *D. takahashii*, *D. eugracilis*, and *D. ananassae*, all have an oviposition preference for rotten fruit (Karageorgi et al., 2017). *D. suzukii* has both physical and behavioral traits that allow it to selectively target ripe fruit as an oviposition substrate (Atallah et al., 2014). Morphologically, *D. suzukii* has evolved an enlarged, serrated ovipositor allowing females to puncture hard surfaces and insert their eggs into ripe fruit. Behaviorally, they have evolved the ability to seek out and selectively target ripe fruits for oviposition through changes in multiple sensory systems (Karageorgi et al., 2017). Thus, the exploitation of the ripe fruit niche by *D. suzukii* requires orchestrated changes at multiple biological levels. Investigating the behavioral and molecular underpinnings of these changes will advance our understanding of the forces and mechanisms that drove *D. suzukii*'s evolution into an invasive pest.

Adaptive shifts in host preference, such as that described for *D. suzukii*, are often mediated through sensory system evolution. Changes in the function and sequence of chemoreceptor genes – including odorant receptors (ORs), ionotropic receptors (IRs), and gustatory receptors (GRs) – and mechanosensory receptor genes (MRs) underlie various species-specific host preference differences in insects (Auer et al., 2020; Dekker et al., 2006; Goldman-Huertas et al., 2015; Karageorgi et al., 2017; Mansourian et al., 2018; Vosshall and Stocker, 2007). For example, modifications to sensory receptor genes are linked to the transition to herbivory in *Scaptomyza flava* (Goldman-Huertas et al., 2015), the oviposition preference for morinda fruits (*Morinda citrafolia*) in *D. sechellia* (Auer et al., 2020; Dekker et al., 2006), and the specialization on marula fruit in ancient *D. melanogaster* (Mansourian et al., 2018). Additionally, through knockout experiments in *D. melanogaster*, sensory gene function has been linked to various behaviors relevant to *D. suzukii* pest activity, including preference of acetic acid containing oviposition sites (Joseph et al., 2009), the avoidance of stiff substrates (Jeong et al., 2016; Zhang et al., 2020, 2016), and the detection of substances that are at different concentrations in ripe and rotten fruit – such as CO_2, acetic acid, and sugar (Fujii et al., 2015; Kwon et al., 2007; Rimal et al., 2019).

While progress has been made in understanding the evolution of olfactory genes in *D. suzukii* (Keesey et al., 2015; Ramasamy et al., 2016), very little is known about the evolutionary history of other sensory genes in this system, despite *D. suzukii*'s oviposition site preference being mediated via multiple sensory systems (Karageorgi et al., 2017). Finally, studies of adaptive sensory gene evolution in *D. suzukii* often focus only on changes to the coding sequence of these genes, despite differential gene expression playing a prominent role in the evolution of adaptive phenotypes (Carroll, 2005; Jones et al., 2012; Phifer-Rixey et al., 2018; Wray, 2007). For example, changes in expression of ORs and odorant-binding proteins in the olfactory organs of *D. sechellia* are thought to in part mediate this species' specialization on morinda fruits (Kopp et al., 2008).

Although the phenotypic and behavioral innovations leading to the pest status of *D. suzukii* are overall well defined, the specific sensory cues used by *D. suzukii* to target ripe fruits as well as the molecular changes accompanying these sensory changes remain unknown. Here we examine these knowledge gaps by investigating the behavioral, genomic, and gene regulatory mechanisms underlying the pest activity of *D. suzukii.*

First, we provide new insights into the stepwise evolution of ripe fruit preference in *D. suzukii* through the in-depth behavioral and genomic examination of two closely related species, *D. subpulchrella* and *D. biarmipes*. Second, we identified key sensory cues of ripe and rotten fruit differentially processed by *D. suzukii, D. subpulchrella, D. biarmipes* and *D. melanogaster* in the context of egg-laying preference. Third, to infer the most recent changes in genome content in *D. suzukii*, we sequenced the genome of the closely related species, *D. subpulchrella,* and performed comparative genomic analyses. Lastly, we identified candidate genes involved in *D. suzukii*'s ability to seek out and target ripe fruits through population level analyses of olfactory, gustatory, and mechanosensory receptor genes with differential expression and signatures of positive selection in *D. suzukii* as compared to *D. subpulchrella, D. biarmipes* and *D. melanogaster*. We provide a view, from multiple levels of analysis, of the origin of pest activity in *D. suzukii*, indicating important sensory cues used by this species during egg-laying, and the gene expression and genomic changes potentially underlying this novel pest behavior.

RESULTS AND DISCUSSION

Ripe fruit preference in *D. suzukii* evolved after the split with *D. subpulchrella.*

To clarify the evolutionary history of *D. suzukii*'s oviposition behavior, we built upon previous work that established a step wise evolution of ripe fruit oviposition preference in *D. suzukii,* with *D. melanogaster* preferring rotten fruit and *D. biarmipes* showing an equal preference for ripe and rotten fruit (Karageorgi et al., 2017) by measuring the oviposition preference of *D. suzukii*'s sister species, *D. subpulchrella*. It was previously hypothesized that *D. subpulchrella* prefers ripe fruit for oviposition, as *D. suzukii* does (Karageorgi et al., 2017), because they share the trait of an enlarged ovipositor and the ability to lay eggs in ripe fruits (Atallah et al., 2014). However, this assumption has not been empirically tested before this study. To test this hypothesis, we placed female flies in a cage with both a ripe and rotten whole strawberry and allowed them to lay eggs overnight. Afterwards, the number of eggs laid in each fruit was counted and an oviposition preference index (OPI) was calculated (Figure 1A, supplementary file 1).

We recapitulated the oviposition preference results for *D. suzukii*, *D. biarmipes*, and *D, melanogaster*, and found that, contrary to the above hypothesis, *D. subpulchrella* has no distinct

preference for ripe or rotten fruit, displaying an intermediate oviposition behavior similar to *D. biarmipes* (OPI = 0.196 ± 0.138SEM) (Figure 1B).

To investigate the relative roles of stiffness and chemosensory differentiation in driving the intermediate preference of *D. subpulchrella*, we measured the oviposition preference of a cut-ripe vs. rotten strawberry for both *D. suzukii* and *D. subpulchrella* (Figure S1A). While both species can puncture and lay eggs in ripe fruit, *D. suzukii* can utilize a wider range of stiff egg-laying substrates as demonstrated by their ability to pierce the skin of grapes, which *D. subpulchrella* cannot do (Atallah et al., 2014). It was previously established that *D. biarmipes* and *D. melanogaster* cannot puncture ripe fruits, so we did not measure them here (Karageorgi et al., 2017). If *D. subpulchrella* oviposition site choice is not based on stiffness, we would expect a similar result to our whole fruit assay, in which *D. subpulchrella* equally prefers cut-ripe and rotten fruit. We found that *D. suzukii* still preferred the ripe fruit (Wilcoxon signed rank test, P =0.0004), while *D. subpulchrella* displayed no significant preference for the ripe or rotten fruit (Wilcoxon signed rank test, P=0.06) (Figure S1B). However, *D. subpulchrella* is trending toward having a ripe fruit preference; the mean OPI for *D. subpulchrella* in this assay (OPI = 0.341 ± 0.166SEM) was higher as compared to their whole fruit OPI (OPI = 0.196 ± 0.138SEM), and *D. suzukii* and *D. subpulchrella* preference distributions were not significantly different from one another (pairwise Wilcoxon Test, P=0.27). This suggests that both stiffness and chemosensory differentiation are involved in *D. subpulchrella* oviposition site choice. Additionally, both *D. suzukii* and *D. subpulchrella* strongly disfavor laying eggs on the exposed, white flesh of the cut fruit, further suggesting that texture differentiation is an important facet of oviposition site choice in these species (Figure S1C).

D. subpulchrella's intermediate preference suggests that ripe fruit preference in *D. suzukii* is due to factors beyond the enlargement of the ovipositor and ability to puncture the skin of ripe fruit and evolved after the split between *D. subpulchrella* and *D. suzukii*. Further, because *D. suzukii* is an invasive pest while *D. subpulchrella* is not, differences between these sister species may point to traits that have contributed to the evolution of pest behavior in *D. suzukii,* and may be important for future efforts in mitigating damage from this invasive pest.

D. suzukii displays a preference for stiff oviposition substrates, an aversion to acetic acid, and lack of preference for sucrose.

Previous studies indicate that *D. suzukii*'s preference for ripe fruit evolved through changes in multiple sensory systems, including the olfactory, gustatory, and mechanosensory systems (Karageorgi et al., 2017; Keesey et al., 2015; Ramasamy et al., 2016). However, the evolutionary history of these sensory changes and the specific sensory cues involved in *D. suzukii*'s oviposition site choice remain unknown. To investigate these questions, we tested the oviposition preference of *D. suzukii, D. subpulchrella, D. biarmipes* and *D. melanogaster* females for four sensory cues that change over the course of fruit maturation from ripening to rotting: ethanol, sucrose, acetic acid, and stiffness (using agarose concentration as a proxy). At early pre-ripe and ripe maturation stages, fruit is firm and contains low levels of ethanol and total acid, both ranging from concentrations of 0 to 1% in strawberries and other fruits (Dudley, 2004; Hidalgo et al., 2012; Montero et al., 1996). In rotten fruit, as fermentation and acidification occur, ethanol and acid concentrations both rise to about 7% for ethanol (Dudley, 2004; Hidalgo et al., 2012), and about 3.5% for acetic acid (Hidalgo et al., 2012). Sugar content is highest in ripe fruit, and differs greatly in various fruit species ranging from concentrations of about 7% to 20% (translating to 200mM to 600mM sucrose) (Basson et al., 2010; Dudley, 2004; Hidalgo et al., 2012; Montero et al., 1996). We tested oviposition preference for each sensory cue at three biologically relevant levels in the context of fruit maturation (see methods) by placing 3-4 females of each species in custom built egg-laying chambers and giving them the choice between two agarose egg-laying substrates: one control and one containing the experimental substrate (Figure 2A, supplementary file 2). Afterwards, the number of eggs laid on each substrate was counted and the OPI was calculated.

When given the choice between 0.25% and 1%, 1.5%, or 2% agarose, *D. suzukii* consistently preferred the stiffer substrate (representative of early fruit maturation stages), while *D. subpulchrella, D. biarmipes* and *D. melanogaster* preferred the softer substrate (Figure 2B, S2A, supplementary file 2, Wilcoxon signed rank test, all P-values <0.01). *D. suzukii*'s striking divergence in stiff substrate preference suggests that the species-specific targeting of stiff oviposition sites is associated with the early fruit stage preference only exhibited by *D. suzukii.* Further, the contrasting stiffness preference of *D. subpulchrella* and *D. suzukii* may explain why *D. suzukii* is able to target a broader range of ripe, soft-skinned fruit despite both species being able to puncture ripe fruits with their enlarged ovipositors (Atallah et al., 2014).

We next measured the oviposition preference for acetic acid and ethanol, which are both products of fermentation that increase as fruit rots, and are attractive oviposition cues for *D. melanogaster* (Azanchi et al., 2013; Dudley, 2004; Eisses, 1997; Joseph et al., 2009; Jouandet and Gallio, 2015; Kacsoh et al., 2013). Using a linear regression approach comparing the difference in preference curve y-intercepts, we found that overall oviposition preference for ethanol did not differ between the four focal species (Figure 2C, see methods for details). This lack of behavioral difference despite clear differences in ripe vs. rotten fruit oviposition preference may be due to the key role of yeast, which converts fruit sugars to ethanol during fermentation, in guiding natural oviposition preference. Both *D. suzukii* and *D. melanogaster* display yeast-mediated oviposition preference, with yeast being a major attractant, more so than fruit volatiles, for *D. melanogaster* (Becher et al., 2012), and *D. suzukii* exhibiting competition dependent yeast attraction, choosing to oviposit in substrates without yeast only when other species are present (Kidera and Takahashi, 2020).

D. melanogaster showed a strong preference for acetic acid at each concentration tested (Wilcoxon signed rank test, all P-values <0.001), whereas *D. suzukii, D. subpulchrella,* and *D. biarmipes* avoided acetic acid at high concentrations, which are representative of late fruit maturation stages (Figure 2D, S2C, supplementary file 2, Wilcoxon signed rank test at 3.5% acetic acid, all P-values <0.01). The preference for acetic acid potentially represents a unique shift in preference for *D. melanogaster,* as opposed to a loss of preference in the *D. suzukii* lineage, as other species in the *D. melanogaster* subgroup, including *D. yakuba*, *D. simulans* and *D. mauritiana*, have a decreased tolerance of acetic acid (McKenzie and McKechnie, 1979; Montooth et al., 2006). Investigating the acetic acid oviposition preference of more species within and outside of the *D. melanogaster* subgroup may help elucidate the role of acetic acid avoidance in conferring ripe vs. rotten fruit preference.

Lastly, we tested the oviposition preference for sucrose in each of the four species. We found that while *D. melanogaster* and *D. biarmipes* have a preference for sucrose at each concentration measured (Wilcoxon signed rank test, all P-values <0.01), *D. suzukii* and *D. subpulchrella* show no preference or aversion to sucrose, with *D. suzukii* having no preference at each concentration measured (Wilcoxon signed rank test, all P-values >0.05), and *D. subpulchrella* having no preference at 400mM and 600mM sucrose (Wilcoxon signed rank test, all P-values >0.05) (Figure 2E, S2D, supplementary file 2). Because sugar increases during

ripening, high sugar content indicates that rotting will begin imminently, perhaps explaining why *D. melanogaster* chooses high sugar substrates despite the fact that their preferred substrate of rotten fruit contains less sugar than ripe fruit. Similarly, *D. suzukii*'s indifference towards sucrose may be associated with their transition towards ovipositing on early fruit maturation stages. While in a two choice scenario *D. suzukii* prefers ripe fruit (higher sugar) over rotten fruit (lower sugar), when given the option of earlier maturation stages, they equally target pre-ripe and ripe fruits for egg-laying (Karageorgi et al., 2017). Sugar is still relatively low during pre-ripe stages (Basson et al., 2010; Montero et al., 1996), suggesting that the loss of sucrose preference in *D. suzukii* could be associated with the selection of early fruit stage oviposition sites. It was previously reported that the chemical composition and contrasting stiffness of ripe and rotten fruit together explain the difference in oviposition preference in *D. suzukii*, *D. biarmipes*, and *D. melanogaster* (Karageorgi et al., 2017). Here, we have identified discrete differences in the roles of sensory cues associated with the fermentation and acetification process of fruit rotting in guiding egg-laying decisions in *D. suzukii* as compared to closely related, non-pest species, *D. subpulchrella* and *D. biarmipes*, as well as *D. melanogaster.*

Sequencing, assembly, and annotation of the *D. subpulchrella* genome.

The results from our phenotypic assays suggesting strongly anchored behavioral differences between species motivated a deeper study of the genetic factors underlying these behavioral differences. In order to apply comparative genomic and genetic approaches, we generated a near-chromosomal level assembly of the *D. subpulchrella* genome using PacBio sequencing (see methods). The genome size is about 265 megabases (Mb), and has a contig N50 of 11.59Mb. Specifically, the longest 6 contigs are 29.67 Mb, 29.50 Mb, 26.21 Mb, 22.17 Mb, 20.23 Mb, and 11.59 Mb, accounting to a total of 139.38 Mb (for details see Table S1). We assessed the gene content of the *D. subpulchrella* genome and found that 98.11% (2746 out of 2799) of the Diptera BUSCO genes are present in the genome, among which, 97.43% (2727) are complete and single-copy genes. When using the 303 BUSCO eukaryota genes, 302 complete genes were found in the genome. This suggests we have assembled a highly complete genome with relatively low levels of redundancy. We then performed three rounds of genome annotation by training the annotation program using MAKER2. In total, we annotated 15,225 genes. Among which, 13,435 genes have reciprocal best hits in *D. suzukii*. We used this gene set for

downstream comparative genomic and transcriptomic analyses. This high-quality genome makes it possible to study the genomic differences and genome evolution of *D. suzukii* and *D. subpulchrella,* and how they compare to other closely related species.

The genome and assembly of *D. subpulchrella* is now available at NCBI through GCF_014743375.2 or JACOEE01. In total, 15,028 protein-coding genes were annotated, which is very similar to our MAKER2 annotation. 29,037 transcripts were annotated with a median length of 1.9kb, which is similar to the median transcript length of *D. melanogaster*. The median number of transcripts per gene was 1.67, and the median number of exons per transcript was 6.16. In addition, a total of 2481 non-coding genes were annotated. We found that 23.95% of the genome was repetitive sequences using RepeatMasker, which is considerably higher than other *Drosophila* species such as *D. melanogaster* (Kaminker et al., 2002), *simulans* species complex (Chakraborty et al., 2020), and *D. hydei* (Zhao and Begun, 2017). Repetitive regions were comprised of 14.09% retroelements, 0.41% DNA transposons, and 3.01% simple repeats, among other types of repetitive sequences. Notably, 6.82% belongs to the Gypsy family, and 1.33% belongs to R1/LOA/Jockey retrotransposons; it would therefore be an interesting future direction to investigate if the telomere elongation mechanism of *D. subpulchrella* is similar to *D. biarmipes* (Saint-Leandre et al., 2019).

Adaptive evolution of sensory receptors implicated in *D. suzukii* oviposition site preference.

Our behavioral analyses show that changes along the *D. suzukii* lineage, in both chemosensory and mechanosensory systems, are involved in the stepwise transition to ripe fruit preference in *D. suzukii*. Therefore, to investigate the genetic changes that lead to *D. suzukii*'s unique oviposition behavior, we analyzed the repertoire of *Drosophila* olfactory, gustatory, and mechanosensory receptor genes for signals of positive selection using population level genomic data from over 200 *D. suzukii* females. Specifically, we performed a McDonald-Kreitman test (MK) to identify candidate odorant receptors (OR), gustatory receptors (GR), ionotropic receptors (IR), and mechanosensory receptors (MR) evolving under positive selection in *D. suzukii* as compared to *D. subpulchrella, D. biarmipes,* and *D. melanogaster* separately (Figure 3). The MK test infers the presence of positive selection by comparing the numbers of fixed and segregating, synonymous and nonsynonymous substitutions in the genomes of a focal population (McDonald and Kreitman, 1991). While there is previous knowledge on ORs evolving under

positive selection in *D. suzukii* as compared to *D. melanogaster* (Ramasamy et al., 2016), our analysis has the additional power of population level data, the additional pairwise comparisons of *D. suzukii* to both *D. biarmipes* and *D. subpulchrella*, and the addition of GRs, IRs, and MRs.

We used three independent methods to perform the MK test (see methods), and consistently identified about 3000 genes evolving under positive selection in *D. suzukii*, as compared to the other three focal species. This number is very large compared to positively selected genes in other *Drosophila* species when inferred through whole genome and population level genomic analyses, which range from 500-1000 positively selected genes (Begun et al., 2007; Langley et al., 2012; Zhao and Begun, 2017). Specifically, we found that d_N/d_S is significantly larger than p_N/p_S, and that both d_N and d_S are large (Figure S3). Since *D. suzukii* recently invaded North America, its evolutionary history suggests that the over-representation of positively selected genes may be caused by the bottleneck of invasion and the subsequent increase in population size and likely effective population size (Eyre-Walker, 2002; McDonald and Kreitman, 1991). Even if the number of genes under positive selection is overestimated, one would expect that there is no bias in which gene categories are enriched for signals of selection. For the majority of species pairwise comparisons between the four focal *Drosophila* species, the sensory receptors analyzed are evolving under positive selection in *D. suzukii* to a greater degree than other regions of the genome (Figure 3, Figure S4). This overrepresentation for signals of positive selection in olfactory, gustatory, and mechanosensory receptors suggest that these genes are at least partly contributing to adaptive evolution in *D. suzukii*. On the other hand, there is also a likelihood of false negative results, and sensory genes that are not significant in our MK test may still be important for adaptive evolution, as changes to a small number of amino acids can cause strong shifts in receptor affinity and specificity, a signal that would not be captured by our analysis. Thus, we focus on identifying candidate sensory genes that show expression divergence or adaptive gene evolution, rather than analyzing them as a whole.

Receptors that are under positive selection in *D. suzukii* in each of the three pairwise species comparisons may underlie *D. suzukii*'s novel oviposition behavior (Figure 3). Such genes include *Or22a*, which is involved in host choice evolution in various *Drosophilid* species (Auer et al., 2020; Goldman-Huertas et al., 2015; Mansourian et al., 2018), *Or85a,* a gene implicated in *D. sechellia*'s specialization on morinda fruit (Auer et al., 2020) that is also thought to either be a pseudogene (Hickner et al., 2016) or have changed function in *D. suzukii* (Ramasamy et al.,

2016), and *Or85d*, which is linked to the detection of yeast volatiles in *D. melanogaster* (Tichy et al., 2008). Gustatory and ionotropic receptors of interest include *Gr63a*, which is involved in the detection of CO_2, a volatile emitted by ripening fruit (Jones et al., 2007; Krause Pham and Ray, 2015; Kwon et al., 2007), and *Ir7a*, an ionotropic receptor linked to acetic acid consumption avoidance in *D. melanogaster* (Rimal et al., 2019). Lastly, mechanosensory receptors of note include *nan*, which is involved in substrate stiffness detection during egg-laying in *D. melanogaster* (Jeong et al., 2016; Zhang et al., 2020), *ppk*, a gene involved in acetic acid attraction during oviposition choice in *D. melanogaster* (Gou et al., 2014), and *Trpγ*, which is also linked to CO_2 detection (Badsha et al., 2012).

Differential expression of sensory receptors implicated in *D. suzukii* oviposition site preference.

To further understand the molecular changes associated with *D. suzukii*'s oviposition preference, we sequenced full transcriptomes and analyzed gene expression data from female adult heads of *D. suzukii*, *D. subpulchrella, D. biarmipes* and *D. melanogaster*. We analyzed expression across all genes and determined differential gene expression in *D. suzukii* as compared to the three other focal species. Significantly differentially expressed genes in each species comparison and the GO enrichment for these gene sets can be found in supplementary file 3. To determine the strongest candidate genes, we then focused on the same set of sensory receptors included in our MK analysis (Table S6), and built upon our positive selection population genomic analysis to curate a final list of genes which exhibit both significant MK tests (in all three species pairwise comparisons), and a significant difference in gene expression (in at least one species comparison). These criteria generated 15 candidate receptor genes potentially underlying *D. suzukii*'s oviposition behavior (Figure 4). These genes include previously mentioned receptors *Or85a, Or85d, Gr63a*, and *Trpγ*, strengthening the potential role of CO_2 detection and host fruit specializing in *D. suzukii*'s ripe fruit preference. This list also includes *Ir56d*, another receptor implicated in the response to carbonation and CO_2 (Sánchez-Alcañiz et al., 2018). Other ORs implicated are *Or10a* and *Or85f*, which are both involved in response to benzaldehydes in *D. melanogaster* (Rollmann et al., 2010), a major volatile emitted by fruits during ripening (Girard and Kopp, 1998). Lastly, candidate MRs include *wtrw*, which is involved in humidity sensation in *D. melanogaster* (Liu et al., 2007), *trpl*, a cation channel

shown to mediate gradual dietary shifts in *D. melanogaster* (Zhang et al., 2013), and *Piezo*, which interacts with the receptor *nan*, mentioned above, to sense substrate stiffness differences in *D. melanogaster* (Zhang et al., 2020).

It is important to note that our results represent data from a single, heterogeneous tissue, and cannot capture many elements of gene expression evolution along the *D. suzukii* lineage. To address this, we analyzed gene expression in the same set of sensory receptors included in our MK analysis (Table S6) using previously published transcriptome data from the abdominal tip of our four focal species (Crava et al., 2020). Overall, fewer sensory receptor genes were expressed in the abdominal tip (Table S7). However, several of our candidate genes, including *Piezo, nan, wtrw, trpl, Or85f,* and *Gr63a* were expressed at different levels among the four focal species, pointing to potentially interesting future directions. Additionally, to ascertain how well our head RNA-seq dataset captures expression information from relevant sensory organs, we analyzed the correlation between our *D. suzukii* head RNA-seq data and published RNA-seq datasets from the proboscis + maxillary palp and antennae of *D. suzukii* females (Paris et al., 2020) among genes in our sensory receptor gene set (Table S6). We found that the relative expression of sensory genes in our *D. suzukii* head RNA-seq dataset and in the proboscis + maxillary and antennae palp datasets were significantly correlated (Spearman's $r = 0.32$ and 0.67, respectively, $P = 0.003$ and 5.5×10^{-12}, respectively) (Figure S5), suggesting that our sample collection method can relatively accurately measure the expression of relevant sensory genes in the context of this study.

While we focus on behavioral and genomic changes to the peripheral sensory system here, we acknowledge that differences in oviposition choice between species could be due to changes in central-brain processing (Seeholzer et al., 2018), and this would be an interesting direction for future studies on *D. suzukii* oviposition preference. In the long-term, it is important to understand how stiffness sensation influences species-specific behavioral differences. We hope the mechanosensory genes observed in this work, such as *Piezo* and *nan,* among other genes (Zhang et al., 2020), will help shed light on the evolution of mechanosensation in this species group.

CONCLUSIONS

Here we present an investigation of the behavioral patterns, sensory modalities, genetic factors and evolutionary forces contributing to the emergence of ripe fruit preference in *D.*

suzukii, a newly invasive and rapidly spreading fruit pest. We show that *D. suzukii* differs from closely related species *D. subpulchrella, D. biarmipes* and *D. melanogaster* in discrete and important ways as it pertains to oviposition preference for whole fruit, and common substances associated with fruit maturation and rotting. As compared to the other *Drosophila* species studied, *D. suzukii* prefers to oviposit in ripe fruit, displays an indifference toward sucrose, an aversion to acetic acid, and a preference for stiff oviposition substrates. The species-specific egg-laying behavior of *D. suzukii* has been shown to be associated with the enlargement and strengthening of the ovipositor allowing females to puncture stiff fruit, a trait shared by its sister species, *D. subpulchrella* (Atallah et al., 2014). Previous work established a stepwise model for the evolution of *D. suzukii* as a pest species in relation to *D. melanogaster* and *D. biarmipes*, focusing on ovipositor size and fruit stage preference (Karageorgi et al., 2017). Our work clarifies and builds upon this model with the addition of empirical fruit preference data in *D. subpulchrella*, a species representing an intermediate step toward the exploitation of ripe fruit as an egg-laying substrate, as well as an in-depth analysis of sensory cues used for the discrimination of fruit maturation stages (Figure 5).

In addition to clarifying the egg-laying preference of *D. subpulchrella*, we generated a high-quality genome for this species. This high-quality genome, together with the genomes of *D. suzukii* (Chiu et al., 2013; Paris et al., 2020) including a PacBio-based assembly (Paris et al., 2020), will benefit evolutionary studies of the *suzukii* species group. Future comparative studies focused on *D. subpulchrella* may help reveal how *D. suzukii* evolved into an invasive pest, while other closely related species did not. Finally, we analyzed the genomic changes associated with *D. suzukii*'s sensory evolution and generated a list of candidate olfactory, gustatory and mechanosensory receptors with signals of both differential gene expression and positive selection (Figure 5). A substantial number of these genes seem to be evolving under positive selection and are differentially expressed in *D. suzukii* as compared to the other species analyzed, despite being recently diverged.

Similar instances of rapid sensory receptor gene evolution can be seen across a wide variety of taxa during the adaptation to new ecological niches. Within the family *Drosophilidae*, sensory receptors have undergone lineage- and species-specific genomic changes driven by positive selection that are linked to ecological specialization (Guo and Kim, 2007). As an example, *Or22a* has undergone several independent molecular evolution events, including

instances of neuronal expansion in the morinda fruit specialist, *D. sechellia* (Auer et al., 2020; Dekker et al., 2006) and the *Pandanus* fruit specialist, *D. erecta* (Linz et al., 2013), and instances of gene deletion in the herbivorous fly, *S. flava* (Goldman-Huertas et al., 2015). Additionally, *Or22a* displays high levels of genetic differentiation among ancient populations of *D. melanogaster* specializing on marula fruit (Mansourian et al., 2018). The implication of rapid sensory receptor evolution in the adaptation to new ecological niches is pervasive beyond the family *Drosophilidae,* such as in the unique pheromone system of orchid bees (Brand et al., 2015), the specialization of human blood feeding in *Aedes aegypti* mosquitos (McBride et al., 2014), and ecotype adaptation across phylogenetically and ecologically diverse mammals (Hayden et al., 2010). This representation across the Kingdom Animalia highlights the importance of sensory receptor gene evolution in mediating ecological shifts.

Previous work on our identified candidate genes in *D. melanogaster* and other *Drosophilid* species suggests that changes in CO_2 detection, stiffness differentiation, rotten fruit volatile sensing, and host choice specialization in part underlie *D. suzukii*'s oviposition preference for ripe fruit (Figure 5). Further work is required to truly understand the functional implications of the genetic changes seen in *D. suzukii*, and the results outlined here are a valuable resource for future studies aimed at understanding the behavioral and molecular basis of pest activity in this species.

METHODS

Fly Stocks and husbandry.

All flies were reared on standard cornmeal medium at 24°C, 55% relative humidity, on a 12-hour light-dark cycle (lights on at 8:00am). Egg-laying experiments were conducted under the same conditions. For behavioral assays we used a set a wild type strains: Canton S for *D. melanogaster*, the genome strain raj3* (Chen et al., 2014) for *D. biarmipes*, #NGN6 from Japan for *D. subpulchrella* (Ehime Stock Center), and the genome strain WT3 (WT3, Chiu et al., 2013) for *D. suzukii*. We tested different lines within species and found all the behaviors are consistent. For example, in *D. melanogaster*, w^{1118} and Canton S show the same results, suggesting that the traits tested here are likely to be fixed in each species. For genomic analyses we used the genome reference strain of *D. melanogaster* (BDSC #2057, Adams et al., 2000), the genome strain of *D.*

biarmipes (raj3*) (Chen et al., 2014), the genome strain of *D. suzukii* (WT3, Chiu et al., 2013), and our lab inbred strain of the wild caught line *D. subpulchrella* (Ehime Stock Center #NGN6).

Egg-laying assays.

Whole fruit 2-choice oviposition assay. Flies were collected as virgins and aged for 7-8 days in food vials containing approximately 10 males and 10 females. For each trial 10 females and 5 males were placed in a mesh experimental cage (10 × 10 × 10 inch, BugDorm 4F2222) which contained both a whole ripe and whole rotten strawberry without anesthesia using an aspirator. Flies were allowed to lay eggs for 19 hours from late afternoon to the next morning, after which the total number of eggs laid in each fruit was counted, and an oviposition preference index (OPI) was calculated as follows: (number of eggs on ripe fruit – number of eggs on rotten fruit)/(number of eggs on ripe fruit + number of eggs on rotten fruit). Ripe strawberries (always of the same variety) were purchased from a local supermarket the day of the experiment, and rotten strawberries (same variety, purchased from the same supermarket) were allowed to rot in a 24°C, 55% relative humidity room for four days prior to the experiment. Only intact fruits without any damage were used in experiments. Between 10 and 12 replicate assays were performed for each species. In total, 45 assays were performed. Cut-ripe fruit vs. rotten fruit assays (Figure S1) were performed in the same way as whole-fruit choice assays, except the ripe fruit was cut in half before the trail, and the exposed flesh was placed facing up in the behavioral chamber.

Substrate 2-choice oviposition assays. For all substrate choice assays flies were collected as virgins, separated by sex, and aged separately for 3-4 days in food vials. 2-3 days prior to the experiment, males and females were placed in a new food vial supplemented with yeast paste (1.5ml ddH_2O + 1g live active yeast) to mate and produce eggs. For each trial 3-4 females were placed in a custom laser cut egg-laying chamber (see description below) containing an agarose pad of the experimental substrate, and an agarose pad of the control substrate. Flies were inserted through a trap door with an aspirator without the use of anesthesia. Flies were allowed to lay eggs for 19 hours, after which the total number of eggs laid on each agarose pad was counted, and the OPI was calculated as follows: (number of eggs on experimental substrate – number of eggs on control substrate)/(number of eggs on experimental substrate + number of eggs on

control substrate). Only assays where flies had laid a total of 10 eggs were included in the final analyses, and between 15 and 32 replicate assays were performed for each species at each concentration point. In total, 905 assays were performed.

Chamber design: Egg-laying chambers for substrate choice assays were custom made using laser cut acrylic plastic. Each chamber contained two separate egg-laying arenas separated by 6 mm of plastic, so two trials could be conducted in one chamber. Each arena contained two wells, into which agarose substrates were poured. Wells measured 32×45×12.7 mm and were divided by 5 mm of plastic. Each arena contained a trap door through which flies could be inserted without the use of anesthesia. A 100×75 mm glass sheet covers the entire chamber to allow light into the chamber, and to prevent flies from escaping.

Sucrose: For sucrose preference assays, experimental substrates were 1% agarose and contained 1% ethanol and increasing concentrations (200mM, 400mM or 600mM) of sucrose (ThermoFisher #S5-3); control substrates were 1% agarose and contained 1% ethanol.

Ethanol: For ethanol preference assays, experimental substrates were 1% agarose and contained 75mM sucrose and increasing concentrations (3%, 5%, and 7%) of ethanol (ThermoFisher #BP2818); control substrates were 1% agarose and contained 75mM sucrose.

Acetic Acid: For acetic acid preference assays, experimental substrates were 1% agarose and contained 75mM sucrose, 1% ethanol and increasing concentrations (1.5%, 2.5%, and 3.5%) of acetic acid (ThermoFisher #A465-250); control substrates were 1% agarose and contained 75mM sucrose and 1% ethanol.

Agarose: For agarose/stiffness preference assays, experimental substrates contained 75mM sucrose, 1% ethanol and increasing concentrations (1%, 1.5%, and 2%) of agarose (Lonza SeaKem LE Agarose #50001); control substrates were 0.25% agarose and contained 75mM sucrose and 1% ethanol.

Statistics. All statistical analyses were performed using R (RStudio version 1.2.1335). For the whole fruit oviposition assays, a Wilcoxon signed rank test was used with the null hypothesis set to 0, signifying no preference. For the substrate gradient preference oviposition assays, a linear regression approach was performed for each substrate using the lme4 package in R to find the overall preference difference between species across the concentrations tested. To determine if the preference curve across the three concentrations differed significantly between the four focal

species, we used the lm function in the lme4 package with the response term of OPI and predictor terms of the cross of concentration and species. The reference group, the species to which the other species are compared, was manipulated using the relevel function in base R to perform pairwise comparisons between the preference curves of each species. Effectively, this sets each of the four different species as the baseline OPI response to the concentration tested and compares this baseline to the other species analyzed. P-values refer to the difference between pairwise comparisons of the y-intercepts of each species' preference curve across the three concentrations. The P-values represent the level of significance for the difference between the slope of each species' regression and 0. Error bars in all figures are mean ± standard error of the mean (SEM) unless otherwise noted.

Genomic analysis

D. subpulchrella genome library preparation and sequencing.

D. subpulchrella inbred line generation. To generate an inbred line for PacBio sequencing, *D. subpulchrella* flies (Ehime Stock Center #NGN6) were inbred via sib-mating for ten generations to generate the strain denominated "*D. subpulchrella* 33 F10 #4".

DNA extraction and Sequencing: We extracted DNA from adult females following the protocol of Chakraborty et al. (Chakraborty et al., 2016). The DNA was sheared using 20 plunges of 21-gauge needle and size selected using the 30kb lower cutoff size on Blue Pippin size selection system (Sage Science). 30kb SMRTbell template library was prepared from the size selected DNA and was sequenced on 4 SMRTcells of Pacific Biosciences Sequel I platform. We also sequenced this sheared DNA sample with 150 bp paired-end library on Illumina Hiseq 4000. All sequencing was performed at UCI GHTF.

Genome assembly: We generated 45.3 Gb of long reads, in which 50% of the sequence is contained within sequences longer than 33.8kb (the longest sequence is 160 kb) and 149.40 million 150 bp paired-end Illumina reads. The reads were corrected and assembled with canu v1.7 using genomeSize=220M (Koren et al., 2017). The assembly was polished twice with arrow (smrtanalysis v5.1.0) using the long reads and twice with Pilon using the Illumina reads (Walker et al., 2014). The size of the final assembly was 265 Mb, 50% of which is contained within reads that are 11.59 Mb or longer (assembly contig N50 11.59 Mb). The genome assembly can be found on NCBI through WGS project# JACOEE01 or BioProject# PRJNA557422. We ran

RepeatMasker against HMM-Dfam_3.2 lib to estimate the number of repetitive sequences in *D. subpulchrella.*

D. subpulchrella genome annotation. To evaluate the genome assembly quality, we used BUSCO (Simão et al., 2015) to estimate the proportion of the 2799 Diptera orthologous genes and the 303 eukaryotic genes that were completely or partially assembled in the genome. We then used the MAKER2 (Holt et al., 2011) genome annotation pipeline for genome annotation. To improve the annotation quality, we trained the HMM for three times before using it for the final annotation (Zhao and Begun, 2017) After that, we used OrthoMCL (Li et al., 2003) to find homologous genes between *D. subpulchrella* and the other *Drosophila* species. For multiple-copy genes, we assigned their orthologous genes by using reciprocal best hits through BLASTP. The NCBI annotation can be found through GenBank assembly accession: GCA_014743375.2 and RefSeq assembly accession: GCF_014743375.2.

McDonald-Kreitman test for positive selection. A high-quality population genome dataset was aligned to the *D. suzukii* genome using bowtie2. After that we called bi-allelic SNPs using ANGSD version 0.920 (Korneliussen et al., 2014). On average the coverage of locations with SNPs is 178. We used bi-alleles that met the following criteria: minimum mapping quality of 30, minimum allele frequency of 0.05, and a minimum coverage larger than 10. We then created alternative references using the set of SNPs. We re-extracted the coding sequence of each gene from alternate references, then re-aligned using PRANK with the –codon function for each *D. suzukii* gene and their orthologous gene in *D. melanogaster*, *D. biarmipes*, and *D. subpulchrella.* We only carried out MK tests for genes that showed at least one variant in each of four categories, polymorphic, fixed, synonymous, and nonsynonymous (Begun et al., 2007). For genes that passed the above criteria we carried out unpolarized McDonald–Kreitman tests using the MK.pl script (Begun et al., 2007), and a version of our own python scripts independently, followed by a Fisher's exact test for each gene within each species pairwise comparison. A third method of MK test using SNPs directly from individuals was also used for confirming the results. For each gene, we estimated the proportion of adaptive amino acid fixations (α) (Smith and Eyre-Walker, 2002) and the Direction of Selection (DoS) index (Stoletzki and Eyre-Walker, 2011).

Lists of ORs, GRs, IRs and MRs were compiled using FlyBase assigned gene groups for *D. melanogaster* and their orthologous genes in the other three species were inferred using OrthoMCL or BLASTP. The ORs, GRs, IRs, and MRs with orthologs in each of the three species, and that met the MK test criteria described above were used for genomic and transcriptomic analyses (Table S6). Short protein sequences do not fit the MK test criteria due to lack of polymorphisms and are therefore not included in our downstream analyses.

Simulations were used to compare the average degree of adaptive evolution occurring in receptor gene groups to the genome-wide average. We randomly sampled gene sets of identical size to the receptor gene set of interest for each separate species comparison (*D. suzukii – D. melanogaster, D. suzukii – D. biarmipes,* and *D. suzukii – D. subpulchrella*) and computed the mean Fisher's exact test P-value for that random gene set. Simulations were run 10,000 times for each set of interest, and P-values represent the proportion of the simulated distribution of means below the observed mean P-value for the receptor gene set of interest.

RNA library preparation, and sequencing. We generated head transcriptomes from female *D. suzukii, D. melanogaster, D. biarmipes,* and *D. subpulchrella.* All individuals were mated and precisely 3-days-old. Female flies were very briefly anesthetized with CO_2 and heads were collected with a clean razor blade. Dissections were performed within a 1-hour window always at the same circadian zeitgeber time (ZT1-ZT2; with light turning on at 8 am, and the dissections being performed between 9 am and 10 pm). We collected 3 biological replicates for each species, each sample contained 15 heads. Dissected heads were immediately transferred into a low retention Eppendorf tube containing 100 μL TRIzol (Invitrogen) and RNA was extracted immediately post dissection.

All RNA extractions were performed according to TRIzol manufacturer protocol and immediately followed by a DNase treatment using the TURBO DNase from Invitrogen. RNA quality was assessed by a Bioanalyzer run of an Agilent Eukaryote Total RNA Pico chip while RNA quantity was measured with a Nanodrop One (ABI). About 1 μg total RNA was used for library preparation. Libraries were fragmented and enriched for mRNA using NEBNext Poly(A)$^+$ Magnetic Isolation Module (NEB #E7490) and prepared using NEBNext Ultra II Directional RNA Library Prep Kit (NEB #E7765) and single indexing from the NEBNext Multiplex Oligos kit (NEB #E7555L) following manufacturer protocol including beads size selection for 200 bp

inserts. Library quality was first assessed on Agilent D1000 ScreenTapes for Tapestation and then by Qubit and Agilent Bioanalyzer. Finally, 150 bp paired-ends libraries were sequenced on an Illumina Nextseq500 platform.

Identification of differentially expressed sensory receptor genes. Adaptors and low-quality bases from RNA-seq reads were trimmed using Trimmomatic (Bolger et al., 2014) using the setting LEADING:1 TRAILING: 1 SLIDINGWINDOW:20:25 and MINLEN:36. Bowtie2 (Langmead and Salzberg, 2012) was then used to align reads to the reference genome of the species being analyzed. Gene and transcript expression levels (TPM: Transcripts per million) were then quantified using StringTie (Pertea et al., 2015). We then obtained a list of homologous genes of *D. suzukii, D. biarmipes,* and *D. subpulchrella* using OrthoMCL and reciprocal best hits. To compare gene expression between replicates from different species we used TMM (trimmed mean M-values) normalized TPM values. TMM normalization was implemented with the R package edgeR (Robinson et al., 2010). We then conducted a Log_2 transformation across all replicates and calculated a P-value using a Student's *t*-test between *D. suzukii* and each of the other focal species to determine if each gene is differential expressed between two species. We specifically queried the expression patterns of sensory receptor genes inferred by homology with *D. melanogaster* sensory receptor genes extracted from FlyBase, using the same gene list as that described for the MK test above (Table S6) (Thurmond et al., 2019). GO enrichment of significantly differentially expressed genes ($P < 0.01$) was performed using PANTHER (Mi et al., 2019).

Evaluation of sensory receptor gene expression in other relevant tissues. Raw RNA-seq reads from the female abdominal tip of the four focal species were downloaded from the Genbank SRA database (BioProject# PRJNA526247) (Crava et al., 2020). Raw reads of adult female proboscis + maxillary palp and female antennae for *D. suzukii* were downloaded from NCBI SRA SRR10716767 and SRR10716770, respectively (Paris et al., 2020). Reads were aligned and analyzed similarly to that described above, with the only difference that no statistical analysis was performed because the data do not have biological replicates.

Correlation between the head RNA-seq dataset and the maxillary palp + proboscis and antennae RNA-seq datasets was done by first ranking the expression of sensory receptor genes

(Table S6) in each of the three datasets. Correlation of the rankings was calculated using the Spearman correlation coefficient in R. Genes that are not expressed were ranked as 1. We used rankings to compare these datasets because the relative raw expression levels could be influenced by technical differences that do not reflect biologically meaningful information.

DATA AVAILABILITY

All single-molecule sequence data and RNA-seq data have been deposited to the NCBI Sequence Read Archive (SRA) and can be found under BioProject accession PRJNA557422. The *D. subpulchrella* genome assembly has been deposited in the NCBI Assembly database under accession JACOEE01. The vcf file for the population genome data can be found in figshare: https://doi.org/10.6084/m9.figshare.c.5237618. The genomes and SNPs used in the MK analysis, and raw behavioral data can be found at the GitHub page https://github.com/LiZhaoLab/D.suzukii_genomes_and_analysis.

ACKNOWLEDGEMENTS

The authors are grateful for the help from many scientists: Vikram Vijayan and Gaby Maimon for help with design and construction of chambers for egg-laying assays used in Figure 2 and Figure S2, and for helpful comments and suggestions; Precision Instrumentation Technologies (PIT) at Rockefeller for help with construction of behavioral chambers; Samuel Khodursky for suggestions on the gene expression analysis; Clara Drew for help with the statistical analyses; the Ehime Stock Center and Dr. Masayoshi Watada from Ehime University for the help with fly stocks; and members of the Zhao lab for helpful discussions. We thank Terence Murphy and Françoise Thibaud-Nissen from NIH Eukaryotic Genome Annotation team for their help with annotation and making the data readily available for the general community.

AUTHOR CONTRIBUTION

S.M.D, L.Z., and N.S. conceived the study. S.M.D performed the behavioral analyses with the help of M.K. C.B.L and AG performed cut-ripe fruit behavioral experiments for the revision of the manuscript. S.M.D generated the genome strain of *D. subpulchrella* and performed RNA sequencing library construction. M.C. and J.J.E. sequenced the *D. subpulchrella* genome. A.A., K.M.L., and J.C.C. generated the *D. suzukii* population genome data. L.Z., S.M.D., A.G., J.P., and N.S. performed the computational analysis. S.M.D. and L.Z. wrote the manuscript with the input from all authors.

FUNDING

L.Z. was supported by the Robertson Foundation, a Monique Weill-Caulier Career Scientist Award, an Alfred P. Sloan Research Fellowship (FG-2018-10627), a Rita Allen Foundation Scholar Program, and a Vallee Scholar Program (VS-2020-35). M.K. was supported by the Rockefeller University Summer Science Research Program. A.G. was supported by NIH NRSA T32 training grant GM066699. The work was supported by NIH MIRA R35GM133780 (L.Z.), NIH K99GM129411 (M.C.), NIH R01GM123303 (J.J.E), USDA SCRI 2015-51181-24252 (J.C.C.), and USDA SCRI 2020-67013-30976 (J.C.C.).

DECLARATION OF INTERESTS

The authors declare no competing interests.

REFERENCES

Adams, M.D., Celniker, S.E., Holt, R. a, Evans, C. a, Gocayne, J.D., Amanatides, P.G., Scherer, S.E., Li, P.W., Hoskins, R. a, Galle, R.F., et al. (2000). The genome sequence of Drosophila melanogaster. Science *287*, 2185–2195.

Adrion, J.R., Kousathanas, A., Pascual, M., Burrack, H.J., Haddad, N.M., Bergland, A.O., Machado, H., Sackton, T.B., Schlenke, T.A., Watada, M., et al. (2014). Drosophila suzukii: The Genetic Footprint of a Recent, Worldwide Invasion. Mol. Biol. Evol. *31*, 3148–3163.

Atallah, J., Teixeira, L., Salazar, R., Zaragoza, G., and Kopp, A. (2014). The making of a pest: the evolution of a fruit-penetrating ovipositor in *Drosophila suzukii* and related species. Proc. R. Soc. B Biol. Sci. *281*, 20132840.

Auer, T.O., Khallaf, M.A., Silbering, A.F., Zappia, G., Ellis, K., Álvarez-Ocaña, R., Arguello, J.R., Hansson, B.S., Jefferis, G.S.X.E., Caron, S.J.C., et al. (2020). Olfactory receptor and circuit evolution promote host specialization. Nature *579*, 402–408.

Azanchi, R., Kaun, K.R., and Heberlein, U. (2013). Competing dopamine neurons drive oviposition choice for ethanol in Drosophila. Proc. Natl. Acad. Sci. U. S. A. *110*, 21153–21158.

Badsha, F., Kain, P., Prabhakar, S., Sundaram, S., Padinjat, R., Rodrigues, V., and Hasan, G. (2012). Mutants in Drosophila TRPC Channels Reduce Olfactory Sensitivity to Carbon Dioxide. PLoS One *7*, e49848.

Basson, C.E., Groenewald, J.H., Kossmann, J., Cronjé, C., and Bauer, R. (2010). Sugar and acid-related quality attributes and enzyme activities in strawberry fruits: Invertase is the main sucrose

hydrolysing enzyme. Food Chem. *121*, 1156–1162.
Becher, P.G., Flick, G., Rozpedowska, E., Schmidt, A., Hagman, A., Lebreton, S., Larsson, M.C., Hansson, B.S., Piškur, J., Witzgall, P., et al. (2012). Yeast, not fruit volatiles mediate Drosophila melanogaster attraction, oviposition and development. Funct. Ecol. *26*, 822–828.
Begun, D.J., Holloway, A.K., Stevens, K., Hillier, L.W., Poh, Y.-P., Hahn, M.W., Nista, P.M., Jones, C.D., Kern, A.D., Dewey, C.N., et al. (2007). Population Genomics: Whole-Genome Analysis of Polymorphism and Divergence in Drosophila simulans. PLoS Biol. *5*, e310.
Bolger, A.M., Lohse, M., and Usadel, B. (2014). Trimmomatic: a flexible trimmer for Illumina sequence data. Bioinformatics *30*, 2114–2120.
Brand, P., Ramírez, S.R., Leese, F., Quezada-Euan, J.J.G., Tollrian, R., and Eltz, T. (2015). Rapid evolution of chemosensory receptor genes in a pair of sibling species of orchid bees (Apidae: Euglossini). BMC Evol. Biol. *15*, 1–16.
Carroll, S.B. (2005). Evolution at two levels: On genes and form. PLoS Biol. *3*, 1159–1166.
Chakraborty, M., Baldwin-Brown, J.G., Long, A.D., and Emerson, J.J. (2016). Contiguous and accurate de novo assembly of metazoan genomes with modest long read coverage. Nucleic Acids Res. *44*, 147.
Chakraborty, M., Chang, C.-H., Khost, D.E., Vedanayagam, J., Adrion, J.R., Liao, Y., Montooth, K.L., Meiklejohn, C.D., Larracuente, A.M., and Emerson, J.J. (2020). Evolution of genome structure in the Drosophila simulans species complex. BioRxiv 2020.02.27.968743.
Chen, Z.X., Sturgill, D., Qu, J., Jiang, H., Park, S., Boley, N., Suzuki, A.M., Fletcher, A.R., Plachetzki, D.C., FitzGerald, P.C., et al. (2014). Comparative validation of the D. melanogaster modENCODE transcriptome annotation. Genome Res. *24*, 1209–1223.
Chiu, J.C., Jiang, X., Zhao, L., Hamm, C.A., Cridland, J.M., Saelao, P., Hamby, K.A., Lee, E.K., Kwok, R.S., Zhang, G., et al. (2013). Genome of Drosophila suzukii, the spotted wing drosophila. G3 (Bethesda). *3*, 2257–2271.
Crava, C.M., Zanini, D., Amati, S., Sollai, G., Crnjar, R., Paoli, M., Rossi-Stacconi, M.V., Rota-Stabelli, O., Tait, G., Haase, A., et al. (2020). Structural and transcriptional evidence of mechanotransduction in the Drosophila suzukii ovipositor. J. Insect Physiol. *125*, 104088.
Dekker, T., Ibba, I., Siju, K.P., Stensmyr, M.C., and Hansson, B.S. (2006). Olfactory shifts parallel superspecialism for toxic fruit in Drosophila melanogaster sibling, D. sechellia. Curr.

Biol. *16*, 101–109.
Dudley, R. (2004). Ethanol, Fruit Ripening, and the Historical Origins of Human Alcoholism in Primate Frugivory 1. Integr. Comp. Biol. *44*, 315–323.
Eisses, K.T. (1997). The influence of 2-propanol and acetone on oviposition rate and oviposition site preference for acetic acid and ethanol of Drosophila melanogaster. Behav. Genet. *27*, 171–180.
Eyre-Walker, A. (2002). Changing effective population size and the McDonald-Kreitman test. Genetics *162*, 2017–2024.
Fraimout, A., Debat, V., Fellous, S., Hufbauer, R.A., Foucaud, J., Pudlo, P., Marin, J.-M., Price, D.K., Cattel, J., Chen, X., et al. (2017). Deciphering the Routes of invasion of Drosophila suzukii by Means of ABC Random Forest. Mol. Biol. Evol. *34*, 980–996.
Fujii, S., Yavuz, A., Slone, J., Jagge, C., Song, X., and Amrein, H. (2015). Drosophila sugar receptors in sweet taste perception, olfaction, and internal nutrient sensing. Curr. Biol. *25*, 621–627.
Girard, B., and Kopp, T.G. (1998). Physicochemical Characteristics of Selected Sweet Cherry Cultivars. J. Agric. Food Chem. *46*, 471–476.
Goldman-Huertas, B., Mitchell, R.F., Lapoint, R.T., Faucher, C.P., Hildebrand, J.G., and Whiteman, N.K. (2015). Evolution of herbivory in Drosophilidae linked to loss of behaviors, antennal responses, odorant receptors, and ancestral diet. Proc. Natl. Acad. Sci. U. S. A. *112*, 3026–3031.
Gou, B., Liu, Y., Guntur, A.R., Stern, U., and Yang, C.H. (2014). Mechanosensitive neurons on the internal reproductive tract contribute to egg-laying- induced acetic acid attraction in Drosophila. Cell Rep. *9*, 522–530.
Guo, S., and Kim, J. (2007). Molecular evolution of Drosophila odorant receptor genes. Mol. Biol. Evol. *24*, 1198–1207.
Hayden, S., Bekaert, M., Crider, T.A., Mariani, S., Murphy, W.J., and Teeling, E.C. (2010). Ecological adaptation determines functional mammalian olfactory subgenomes. Genome Res. *20*, 1–9.
Hickner, P. V., Rivaldi, C.L., Johnson, C.M., Siddappaji, M., Raster, G.J., and Syed, Z. (2016). The making of a pest: Insights from the evolution of chemosensory receptor families in a pestiferous and invasive fly, Drosophila suzukii. BMC Genomics *17*, 648.

Hidalgo, C., Torija, M.J., Mas, A., and Mateo, E. (2012). Effect of inoculation on strawberry fermentation and acetification processes using native strains of yeast and acetic acid bacteria.
Holt, C., Yandell, M., Adams, M., Celniker, S., Holt, R., Evans, C., Gocayne, J., Amanatides, P., Scherer, S., Li, P., et al. (2011). MAKER2: an annotation pipeline and genome-database management tool for second-generation genome projects. BMC Bioinformatics *12*, 491.
Jeong, Y.T., Oh, S.M., Shim, J., Seo, J.T., Kwon, J.Y., and Moon, S.J. (2016). Mechanosensory neurons control sweet sensing in Drosophila. Nat. Commun. *7*, 1–9.
Jones, F.C., Grabherr, M.G., Chan, Y.F., Russell, P., Mauceli, E., Johnson, J., Swofford, R., Pirun, M., Zody, M.C., White, S., et al. (2012). The genomic basis of adaptive evolution in threespine sticklebacks. Nature *484*, 55–61.
Jones, W.D., Cayirlioglu, P., Grunwald Kadow, I., and Vosshall, L.B. (2007). Two chemosensory receptors together mediate carbon dioxide detection in Drosophila. Nature *445*, 86–90.
Joseph, R.M., Devineni, A. V., King, I.F.G., and Heberlein, U. (2009). Oviposition preference for and positional avoidance of acetic acid provide a model for competing behavioral drives in Drosophila. Proc. Natl. Acad. Sci. U. S. A. *106*, 11352–11357.
Jouandet, G.C., and Gallio, M. (2015). Catching more flies with vinegar. Elife *4*.
Kacsoh, B.Z., Lynch, Z.R., Mortimer, N.T., and Schlenke, T.A. (2013). Fruit flies medicate offspring after seeing parasites. Science (80-.). *339*, 947–950.
Kaminker, J.S., Bergman, C.M., Kronmiller, B., Carlson, J., Svirskas, R., Patel, S., Frise, E., Wheeler, D.A., Lewis, S.E., Rubin, G.M., et al. (2002). The transposable elements of the Drosophila melanogaster euchromatin: a genomics perspective. Genome Biol. *3*, research0084.1.
Karageorgi, M., Bräcker, L.B., Lebreton, S., Minervino, C., Cavey, M., Siju, K.P., Grunwald Kadow, I.C., Gompel, N., and Prud'homme, B. (2017). Evolution of Multiple Sensory Systems Drives Novel Egg-Laying Behavior in the Fruit Pest Drosophila suzukii. Curr. Biol. *27*, 847–853.
Keesey, I.W., Knaden, M., and Hansson, B.S. (2015). Olfactory specialization in Drosophila suzukii supports an ecological shift in host preference from rotten to fresh fruit. J. Chem. Ecol. *41*, 121–128.
Kidera, H., and Takahashi, K.H. (2020). Chemical cues from competitors change the oviposition preference of *Drosophila suzukii*. Entomol. Exp. Appl. *168*, 304–310.

Kopp, A., Barmina, O., Hamilton, A.M., Higgins, L., McIntyre, L.M., and Jones, C.D. (2008). Evolution of gene expression in the Drosophila olfactory system. Mol. Biol. Evol. *25*, 1081–1092.

Koren, S., Walenz, B.P., Berlin, K., Miller, J.R., Bergman, N.H., and Phillippy, A.M. (2017). Canu: Scalable and accurate long-read assembly via adaptive κ-mer weighting and repeat separation. Genome Res. *27*, 722–736.

Korneliussen, T.S., Albrechtsen, A., and Nielsen, R. (2014). ANGSD: Analysis of Next Generation Sequencing Data. BMC Bioinformatics *15*, 356.

Krause Pham, C., and Ray, A. (2015). Conservation of Olfactory Avoidance in Drosophila Species and Identification of Repellents for Drosophila suzukii. Sci. Rep. *5*.

Kwon, J.Y., Dahanukar, A., Weiss, L.A., and Carlson, J.R. (2007). The molecular basis of CO2 reception in Drosophila. Proc. Natl. Acad. Sci. U. S. A. *104*, 3574–3578.

Langley, C.H., Stevens, K., Cardeno, C., Lee, Y.C.G., Schrider, D.R., Pool, J.E., Langley, S.A., Suarez, C., Corbett-Detig, R.B., Kolaczkowski, B., et al. (2012). Genomic Variation in Natural Populations of Drosophila melanogaster. Genetics *192*, 533–598.

Langmead, B., and Salzberg, S.L. (2012). Fast gapped-read alignment with Bowtie 2. Nat. Methods *9*, 357–359.

Li, L., Stoeckert, C.J., and Roos, D.S. (2003). OrthoMCL: identification of ortholog groups for eukaryotic genomes. Genome Res. *13*, 2178–2189.

Linz, J., Baschwitz, A., Strutz, A., Dweck, H.K.M., Sachse, S., Hansson, B.S., and Stensmyr, M.C. (2013). Host plant-driven sensory specialization in *Drosophila erecta*. Proc. R. Soc. B Biol. Sci. *280*, 20130626.

Liu, L., Li, Y., Wang, R., Yin, C., Dong, Q., Hing, H., Kim, C., and Welsh, M.J. (2007). Drosophila hygrosensation requires the TRP channels water witch and nanchung. Nature *450*, 294–298.

Mansourian, S., Enjin, A., Jirle, E. V., Ramesh, V., Rehermann, G., Becher, P.G., Pool, J.E., and Stensmyr, M.C. (2018). Wild African Drosophila melanogaster Are Seasonal Specialists on Marula Fruit. Curr. Biol. *28*, 3960-3968.e3.

Mayr, E. (1960). The emergence of evolutionary novelties. In Evolution after Darwin, p.

McBride, C.S., Baier, F., Omondi, A.B., Spitzer, S.A., Lutomiah, J., Sang, R., Ignell, R., and Vosshall, L.B. (2014). Evolution of mosquito preference for humans linked to an odorant

receptor. Nature *515*, 222–227.
McDonald, J.H., and Kreitman, M. (1991). Adaptive protein evolution at the Adh locus in Drosophila. Nature *351*, 652–654.
McKenzie, J.A., and McKechnie, S.W. (1979). A comparative study of resource utilization in natural populations of Drosophila melanogaster and D. simulans. Oecologia *40*, 299–309.
Mi, H., Muruganujan, A., Huang, X., Ebert, D., Mills, C., Guo, X., and Thomas, P.D. (2019). Protocol Update for large-scale genome and gene function analysis with the PANTHER classification system (v.14.0). Nat. Protoc. *14*, 703–721.
Moczek, A.P. (2008). On the origins of novelty in development and evolution. BioEssays *30*, 432–447.
Montero, T.M., Mollá, E.M., Esteban, R.M., and López-Andréu, F.J. (1996). Quality attributes of strawberry during ripening. Sci. Hortic. (Amsterdam). *65*, 239–250.
Montooth, K.L., Siebenthall, K.T., and Clark, A.G. (2006). Membrane lipid physiology and toxin catabolism underlie ethanol and acetic acid tolerance in Drosophila melanogaster. J. Exp. Biol. *209*, 3837–3850.
Muller, G.B., and Wagner, G.P. (1991). Novelty in Evolution: Restructuring the Concept. Annu. Rev. Ecol. Syst. *22*, 229–256.
Paris, M., Boyer, R., Jaenichen, R., Wolf, J., Karageorgi, M., Green, J., Cagnon, M., Parinello, H., Estoup, A., Gautier, M., et al. (2020). Near-chromosome level genome assembly of the fruit pest Drosophila suzukii using long-read sequencing. Sci. Rep. *10*, 11227.
Pertea, M., Pertea, G.M., Antonescu, C.M., Chang, T.-C., Mendell, J.T., and Salzberg, S.L. (2015). StringTie enables improved reconstruction of a transcriptome from RNA-seq reads. Nat. Biotechnol. *33*, 290–295.
Phifer-Rixey, M., Bi, K., Ferris, K.G., Sheehan, M.J., Lin, D., Mack, K.L., Keeble, S.M., Suzuki, T.A., Good, J.M., and Nachman, M.W. (2018). The genomic basis of environmental adaptation in house mice. PLOS Genet. *14*, e1007672.
Ramasamy, S., Ometto, L., Crava, C.M., Revadi, S., Kaur, R., Horner, D.S., Pisani, D., Dekker, T., Anfora, G., and Rota-Stabelli, O. (2016). The Evolution of Olfactory Gene Families in Drosophila and the Genomic Basis of chemical-Ecological Adaptation in Drosophila suzukii. Genome Biol. Evol. *8*, 2297–2311.
Rimal, S., Sang, J., Poudel, S., Thakur, D., Montell, C., and Lee, Y. (2019). Mechanism of

Acetic Acid Gustatory Repulsion in Drosophila. Cell Rep. *26*, 1432-1442.e4.
Robinson, M.D., McCarthy, D.J., and Smyth, G.K. (2010). edgeR: a Bioconductor package for differential expression analysis of digital gene expression data. Bioinformatics *26*, 139–140.
Rollmann, S.M., Wang, P., Date, P., West, S.A., Mackay, T.F.C., and Anholt, R.R.H. (2010). Odorant receptor polymorphisms and natural variation in olfactory behavior in Drosophila melanogaster. Genetics *186*, 687–697.
Rota-Stabelli, O., Blaxter, M., and Anfora, G. (2013). Drosophila suzukii. Curr. Biol. *23*, R8.
Saint-Leandre, B., Nguyen, S.C., and Levine, M.T. (2019). Diversification and collapse of a telomere elongation mechanism. Genome Res. *29*, 920–931.
Sánchez-Alcañiz, J.A., Silbering, A.F., Croset, V., Zappia, G., Sivasubramaniam, A.K., Abuin, L., Sahai, S.Y., Münch, D., Steck, K., Auer, T.O., et al. (2018). An expression atlas of variant ionotropic glutamate receptors identifies a molecular basis of carbonation sensing. Nat. Commun. *9*, 1–14.
Seeholzer, L.F., Seppo, M., Stern, D.L., and Ruta, V. (2018). Evolution of a central neural circuit underlies Drosophila mate preferences. Nature *559*, 564–569.
Simão, F.A., Waterhouse, R.M., Ioannidis, P., Kriventseva, E. V, and Zdobnov, E.M. (2015). BUSCO: assessing genome assembly and annotation completeness with single-copy orthologs. Bioinformatics *31*, 3210–3212.
Smith, N.G.C., and Eyre-Walker, A. (2002). Adaptive protein evolution in Drosophila. Nature *415*, 1022–1024.
Stoletzki, N., and Eyre-Walker, A. (2011). Estimation of the Neutrality Index. Mol. Biol. Evol. *28*, 63–70.
Thurmond, J., Goodman, J.L., Strelets, V.B., Attrill, H., Gramates, L.S., Marygold, S.J., Matthews, B.B., Millburn, G., Antonazzo, G., Trovisco, V., et al. (2019). FlyBase 2.0: the next generation. Nucleic Acids Res. *47*, D759–D765.
Tichy, A.L., Ray, A., and Carlson, J.R. (2008). A new Drosophila POU gene, pdm3, acts in odor receptor expression and axon targeting of olfactory neurons. J. Neurosci. *28*, 7121–7129.
Vosshall, L.B., and Stocker, R.F. (2007). Molecular Architecture of Smell and Taste in Drosophila . Annu. Rev. Neurosci. *30*, 505–533.
Walker, B.J., Abeel, T., Shea, T., Priest, M., Abouelliel, A., Sakthikumar, S., Cuomo, C.A., Zeng, Q., Wortman, J., Young, S.K., et al. (2014). Pilon: An Integrated Tool for Comprehensive

Microbial Variant Detection and Genome Assembly Improvement. PLoS One *9*, e112963.
Wray, G.A. (2007). The evolutionary significance of cis-regulatory mutations. Nat. Rev. Genet. *8*, 206–216.
Zhang, L., Yu, J., Guo, X., Wei, J., Liu, T., and Zhang, W. (2020). Parallel Mechanosensory Pathways Direct Oviposition Decision-Making in Drosophila. Curr. Biol. *30*, 3075-3088.e4.
Zhang, Y. V., Raghuwanshi, R.P., Shen, W.L., and Montell, C. (2013). Food experience-induced taste desensitization modulated by the Drosophila TRPL channel. Nat. Neurosci. *16*, 1468–1476.
Zhang, Y. V, Aikin, T.J., Li, Z., and Montell, C. (2016). The Basis of Food Texture Sensation in Drosophila. Neuron *91*, 863–877.
Zhao, L., and Begun, D.J. (2017). Genomics of parallel adaptation at two timescales in Drosophila. PLOS Genet. *13*, e1007016.

FIGURES

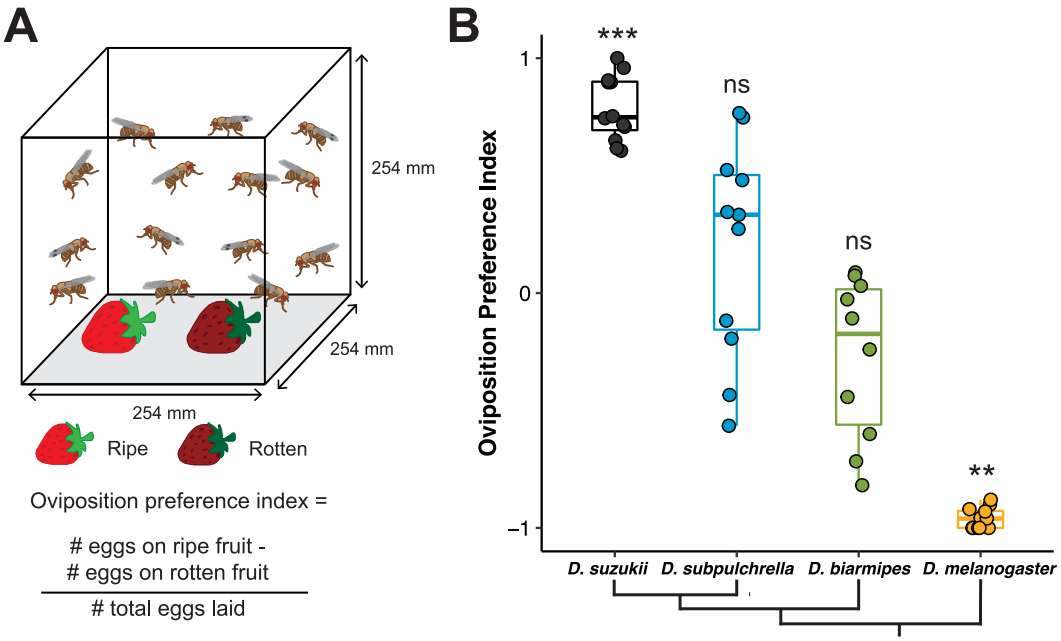

Figure 1. The evolution of ripe fruit preference in *D. suzukii* occurred gradually, with *D. subpulchrella* and *D. biarmipes* as intermediates.
A. Schematic of two-choice oviposition preference assay. 10 females and 5 males were placed in a cage with a ripe and rotten strawberry for 19 hours. Number of eggs on each fruit was then counted.
B. Oviposition preference index of four focal species. *D. suzukii* prefers to oviposit in ripe fruit, *D. subpulchrella* and *D. biarmipes* show no preference for either fruit, and *D. melanogaster* prefers rotten fruit. Each data point represents one experimental trial and data dispersion is represented by a boxplot. Preference P-values were calculated using a Wilcoxon signed rank test against a theoretical value of 0 (no preference). ***, $p \leq 0.001$; **, $p \leq = 0.01$; *, $p \leq 0.05$; ns, $p > 0.05$ for all future figures.

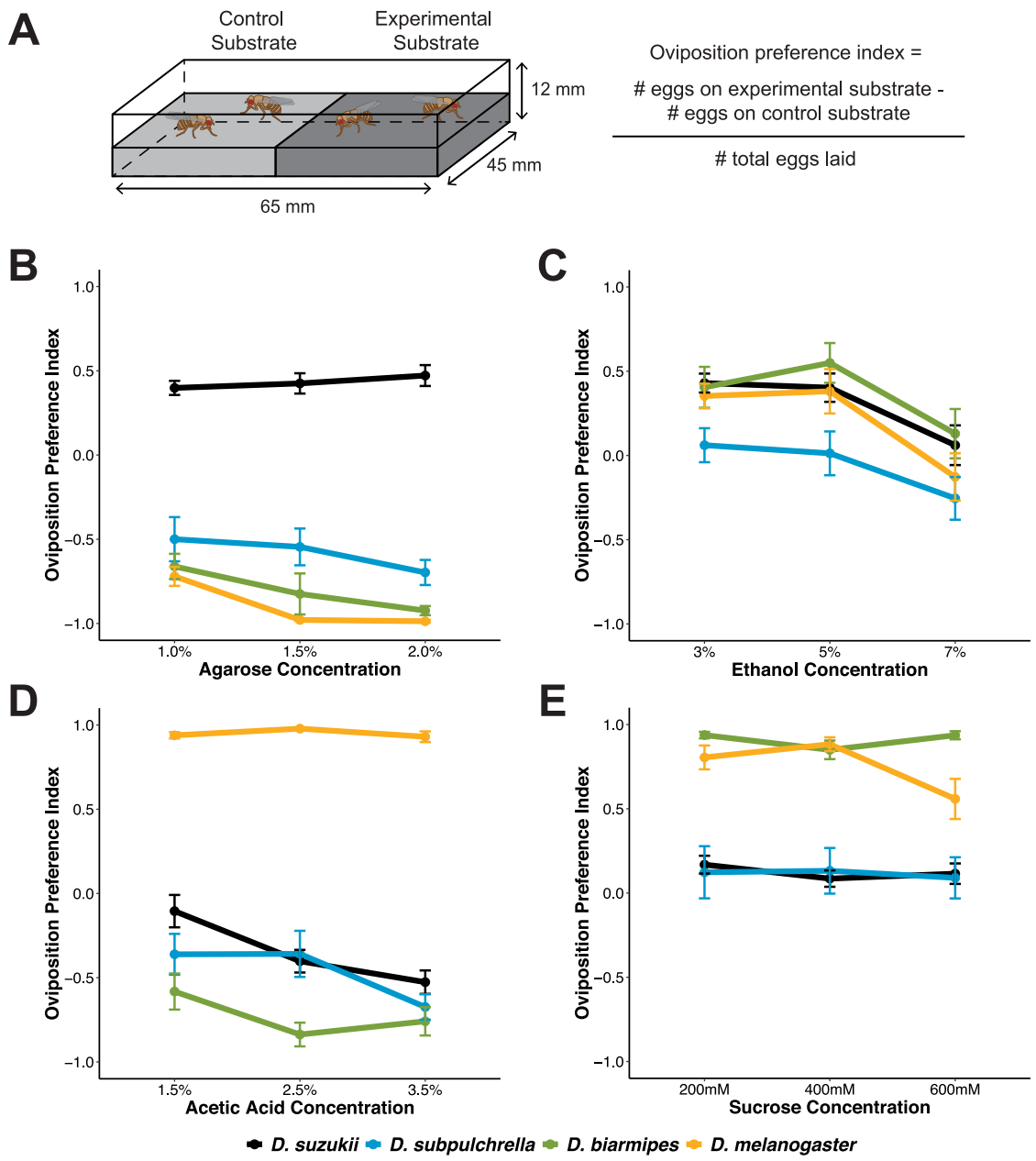
A
Control Substrate
Experimental Substrate
12 mm
45 mm
65 mm
Oviposition preference index =
eggs on experimental substrate - # eggs on control substrate
total eggs laid
B
C
D
E
Oviposition Preference Index
1.0
0.5
0.0
−0.5
−1.0
1.0%
1.5%
2.0%
Agarose Concentration
3%
5%
7%
Ethanol Concentration
1.5%
2.5%
3.5%
Acetic Acid Concentration
200mM
400mM
600mM
Sucrose Concentration
D. suzukii
D. subpulchrella
D. biarmipes
D. melanogaster

Figure 2. Oviposition preference for substrates associated with fruit maturation differ among focal species.

A. Schematic of egg laying chamber for the substrate gradient two-choice oviposition preference assay. 3-4 females were placed in an arena with a choice between two substrates for 19 hours. Number of eggs on each substrate was then counted. Experimental substrate was varying concentrations of either ethanol, sucrose, acetic acid, or agarose. $n \geq 15$ for each species at each concentration. P-values calculated through linear regression analysis through pairwise comparisons of the y-intercepts of each species' preference curve across the three concentrations (see methods). Data points are mean ± SEM.

B. Stiffness preference separated *D. suzukii* from the other three species, as it was the only species that consistently prefers stiffer oviposition substrates. There were significant differences in the preference curves of *D. suzukii* and *D. subpulchrella* (*)*, D. suzukii* and *D. biarmipes* (**)*, and D. suzukii* and *D. melanogaster* (***).

C. Ethanol oviposition preference did not differ between *D. suzukii, D. biarmipes*, or *D. melanogaster*, with all species showing a preference for ethanol at 3% and 5%, and a neutral response to ethanol at 7%. *D. subpulchrella* displayed a neutral response to ethanol at each concentration measured. There were no significant differences in preference curves between any two species.

D. *D. melanogaster* had a strong oviposition preference for acetic acid at each concentration measured, while *D. biarmipes, D. subpulchrella,* and *D. suzukii* had an aversion to acetic acid containing substrates. There were significant differences in the preference curves of *D. suzukii* and *D. biarmipes* (**)*, D. suzukii* and *D. melanogaster* (***)*, D. subpulchrella* and *D. melanogaster* (***)*,* and *D. biarmipes* and *D. melanogaster* (***).

E. *D. suzukii* and *D. subpulchrella* did not show an aversion to or preference for sucrose at any concentration measured, while *D. biarmipes* and *D. melanogaster* prefer sucrose containing substrates. There were significant differences in the preference curves of *D. suzukii* and *D. biarmipes* (***), *D. suzukii* and *D. melanogaster* (***), *D. subpulchrella* and *D. biarmipes* (**), and *D. subpulchrella* and *D. melanogaster* (**).

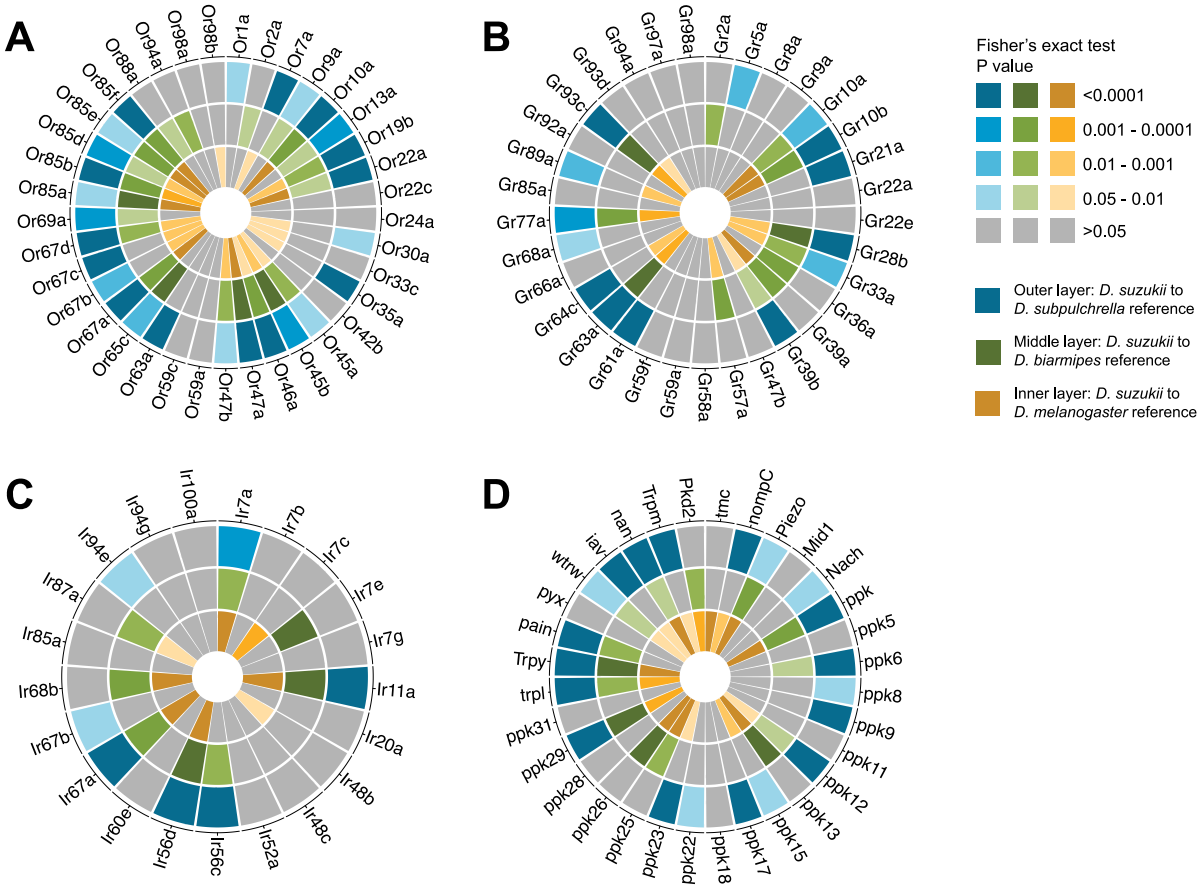

Figure 3. McDonald-Kreitman test for sensory receptors evolving under positive selection in *D. suzukii,* as compared to *D. subpulchrella*, *D. biarmipes,* and *D. melanogaster.*
Odorant receptors (A), gustatory receptors (B), divergent ionotropic receptors (C), and mechanosensory receptors (D) undergoing adaptive evolution in *D. suzukii*. MK test conducted using population data from >200 *D. suzukii* genomes. P-values calculated using Fisher's exact test.

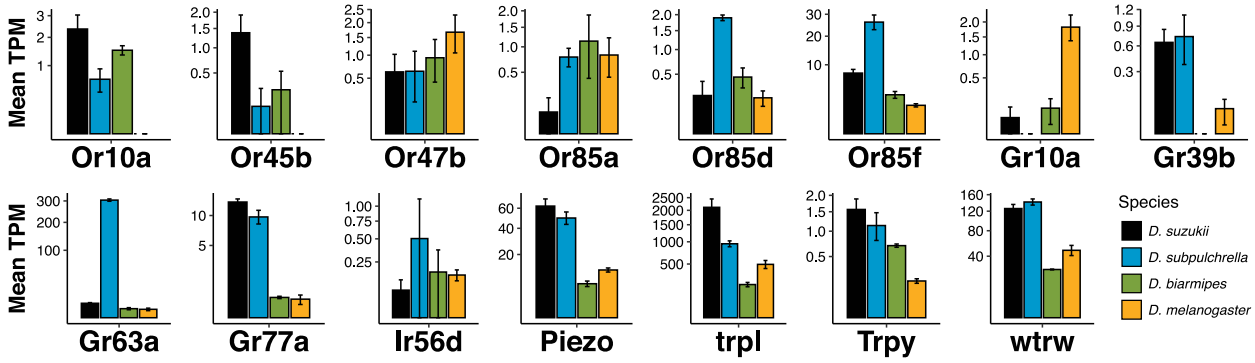

Figure 4. Gene expression of candidate sensory receptors potentially underlying *D. suzukii*'s novel oviposition behavior.
Fifteen candidate ORs, GRs, IRs, and MRs were identified as both evolving under positive selection in D. *suzukii* compared to *D. subpulchrella*, *D. biarmipes,* and *D. melanogaster* and significantly differentially expressed ($P < 0.05$) in at least one species as compared to *D. suzukii* in the gene expression analysis. The y-axes are mean transcripts per million (TPM) normalized between all species and each y-axis is square root transformed. P-values listed in supplementary tables S2-5 and calculated using species pairwise *t*-tests. Histogram bars are mean ± SD.

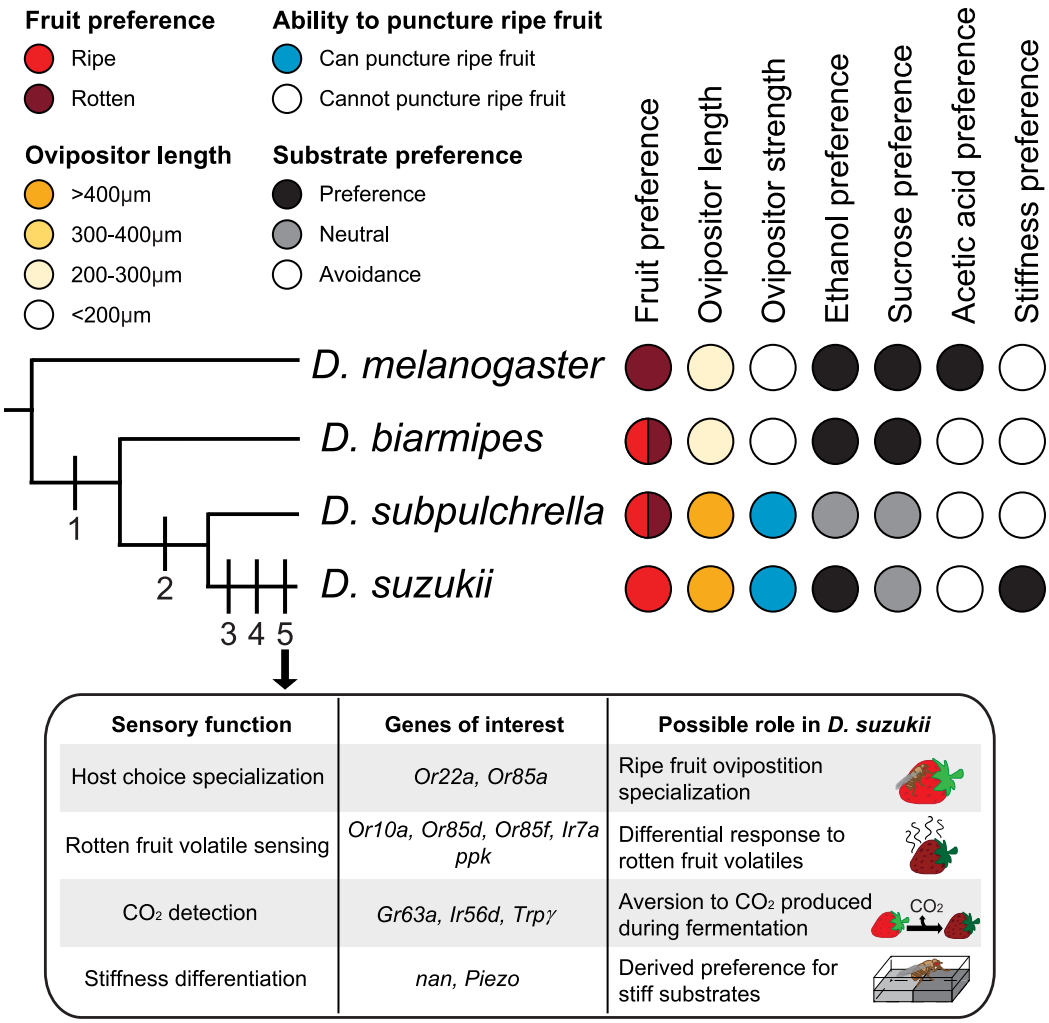

Figure 5. Model of best behavior evolution in *D. suzukii.*
The traits acquired step-wise leading to the specialization on ripe fruit in this model are: 1. Relaxation of rotten fruit preference, 2. Enlarged ovipositor and ability to puncture ripe fruits, 3. Ripe fruit specialization, 4. Preference for stiff substrates, and 5. *D. suzukii*-specific molecular sensory changes (highlighted in the inset table). Ovipositor strength and length data from Atallah et al. 2014.

SUPPLEMENTARY FIGURES & TABLES FOR

Behavioral and genomic sensory adaptations underlying the pest activity of *Drosophila suzukii*

Sylvia M. Durkin[1, 2], Mahul Chakraborty[3], Antoine Abrieux[4], Kyle M. Lewald[4], Alice Gadau[1], Nicolas Svetec[1], Junhui Peng[1], Miriam Kopyto[1], Christopher B. Langer[1], Joanna C. Chiu[4], J.J. Emerson[3], Li Zhao[1,*]

1. Laboratory of Evolutionary Genetics and Genomics, The Rockefeller University, New York, NY 10065, USA

2. Department of Integrative Biology & Museum of Vertebrate Zoology, University of California, Berkeley, Berkeley, CA, USA

3. Department of Ecology and Evolutionary Biology, University of California, Irvine, CA, USA

4. Department of Entomology and Nematology, College of Agricultural and Environmental Sciences, University of California, Davis, CA, USA

*Correspondence to: lzhao@rockefeller.edu

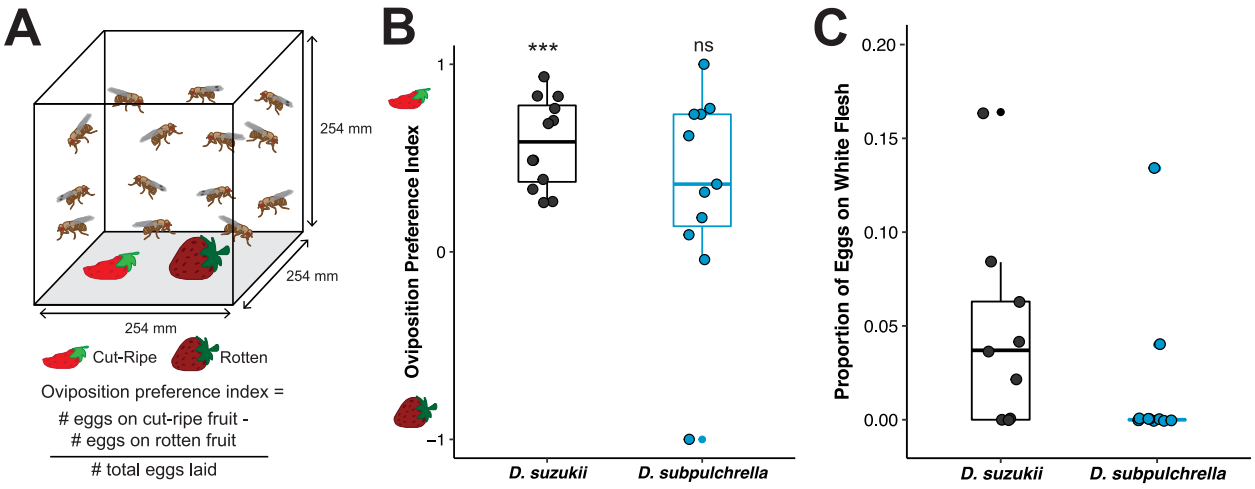

Figure S1. Cut-ripe vs. rotten fruit preference in *D. suzukii* and *D. subpulchrella*.
A. Schematic of two-choice oviposition preference assay. 10 females and 5 males were placed in a cage with a cut-ripe (with flesh facing up) and rotten strawberry for 19 hours. Number of eggs on each fruit was then counted. B. Oviposition preference for cut-ripe fruit (positive OPI) vs. rotten strawberry (negative OPI) in *D. suzukii* and *D. subpulchrella*. C. Proportion of eggs laid on the white, exposed flesh of the cut strawberry in comparison to the intact skin of the ripe strawberry. Each data point represents one experimental trial and data dispersion is represented by a boxplot. Preference P-values were calculated using a Wilcoxon signed rank test against a theoretical value of 0 (no preference). ***, $p \leq 0.001$; **, $p \leq = 0.01$; *, $p \leq 0.05$; ns, $p > 0.05$ for all future figures.

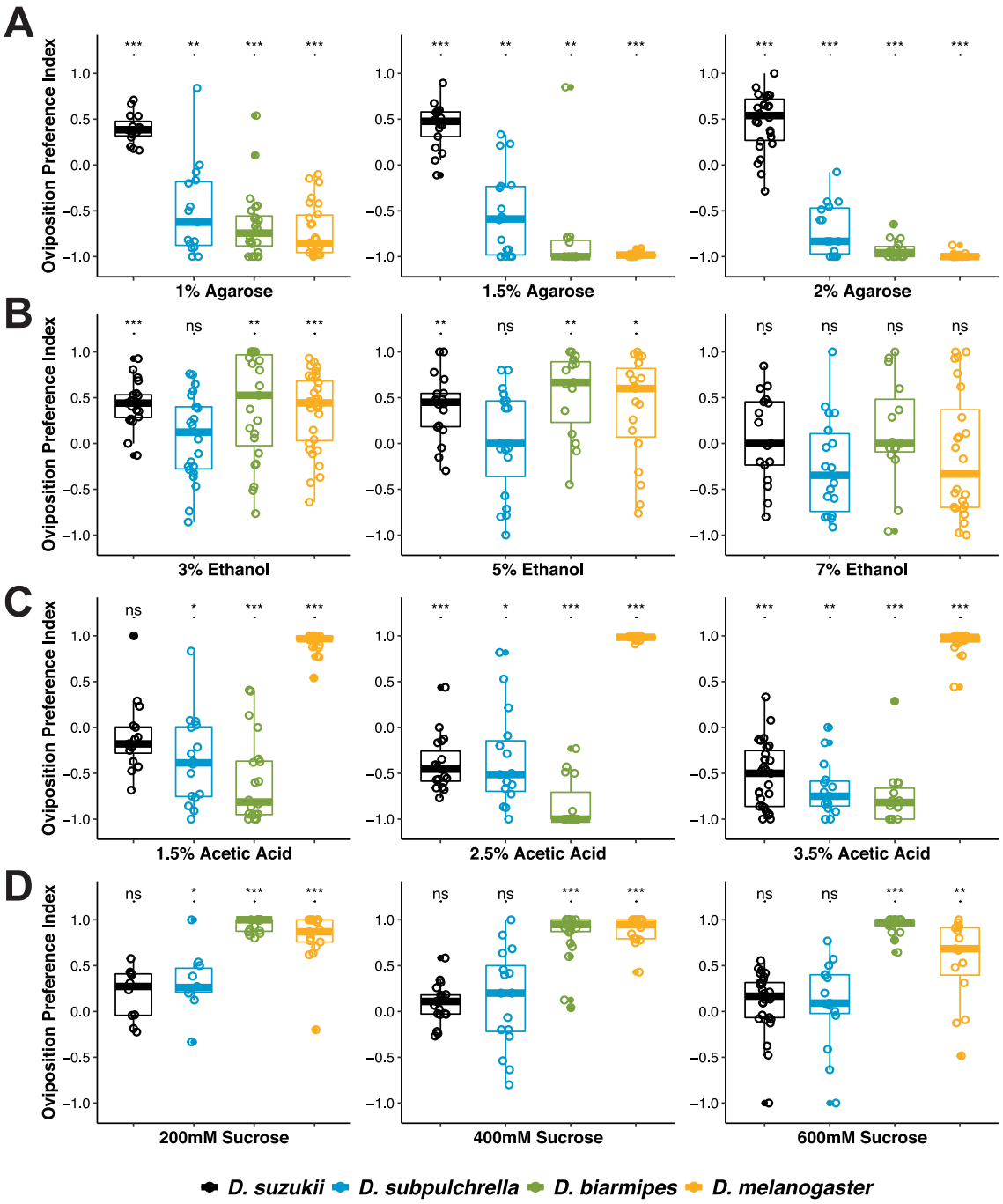

Figure S2. Oviposition preference at each concentration point.
Species specific oviposition preference at each separate concentration tested of agarose (A), ethanol (B), acetic acid (C) and sucrose (D). Each data point represents one experimental trial and data dispersion is represented by a boxplot. Preference P-values were calculated using a Wilcoxon signed rank test against a theoretical value of 0 (no preference).

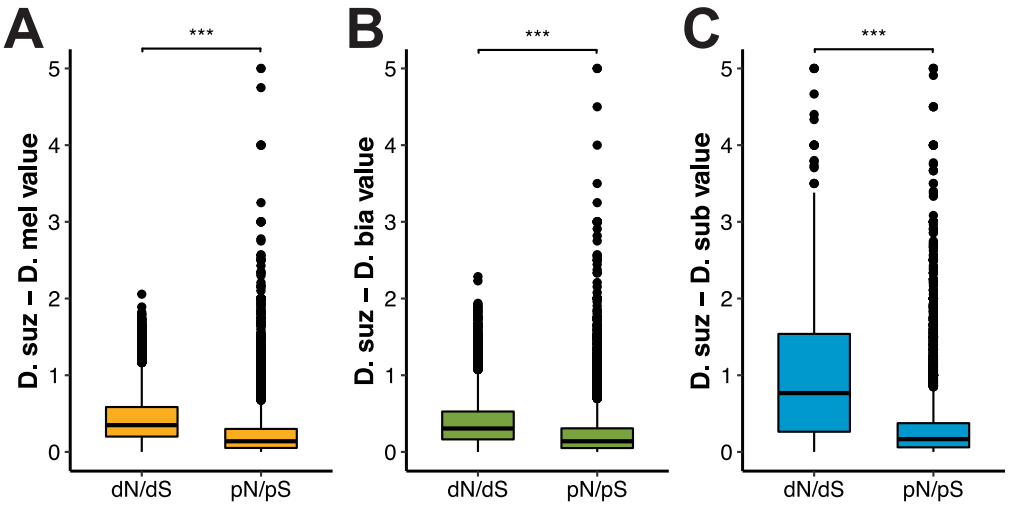

Figure S3. Distribution of d_N/d_S and p_N/p_S from genome wide McDonald-Kreitman test.
d_N/d_S is significantly larger than p_N/p_S across the genome in all three species pairwise comparisons: *D. suzukii* to *D. melanogaster* (A), *D. suzukii* to *D. biarmipes* (B), and *D. suzukii* to *D. subpulchrella* (C). Y-axes have a cutoff of 5. However, all values were included for statistical analyses and P-values were calculated through pairwise *t*-tests.

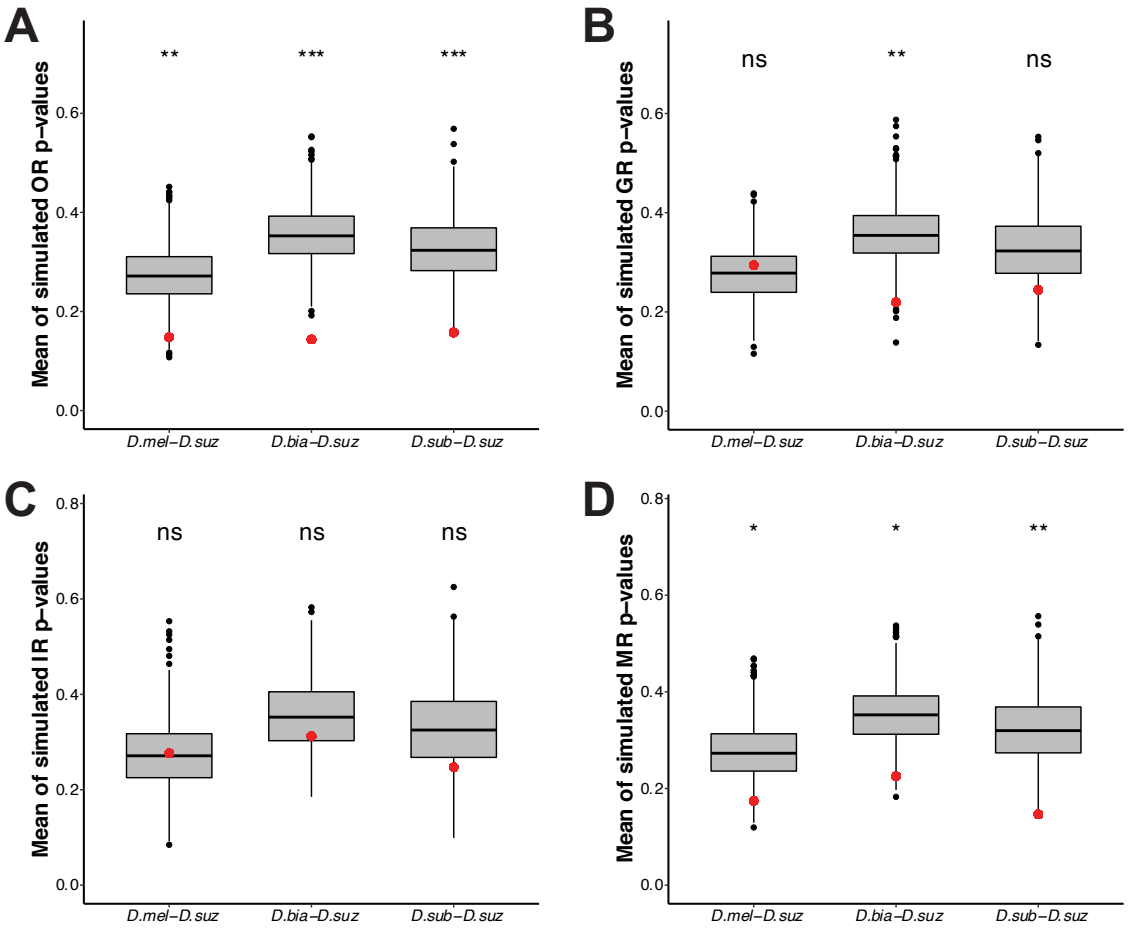

Figure S4. Sensory receptor genes are evolving under positive selection to a greater extent than the genome as a whole.
To generate distributions of simulated mean p-values for ORs (A), GRs (B), IRs (C) and MRs (D) for each species comparison, a random group of genes of the same number as the group of sensory receptor gene groups was selected 10,000 times, and the mean of the random gene group was plotted. Red dots represent the actual mean P-value for the sensory receptor gene group within each species comparison. Significance labels represent the proportion of the distribution lower than the actual mean P-value (red dot).

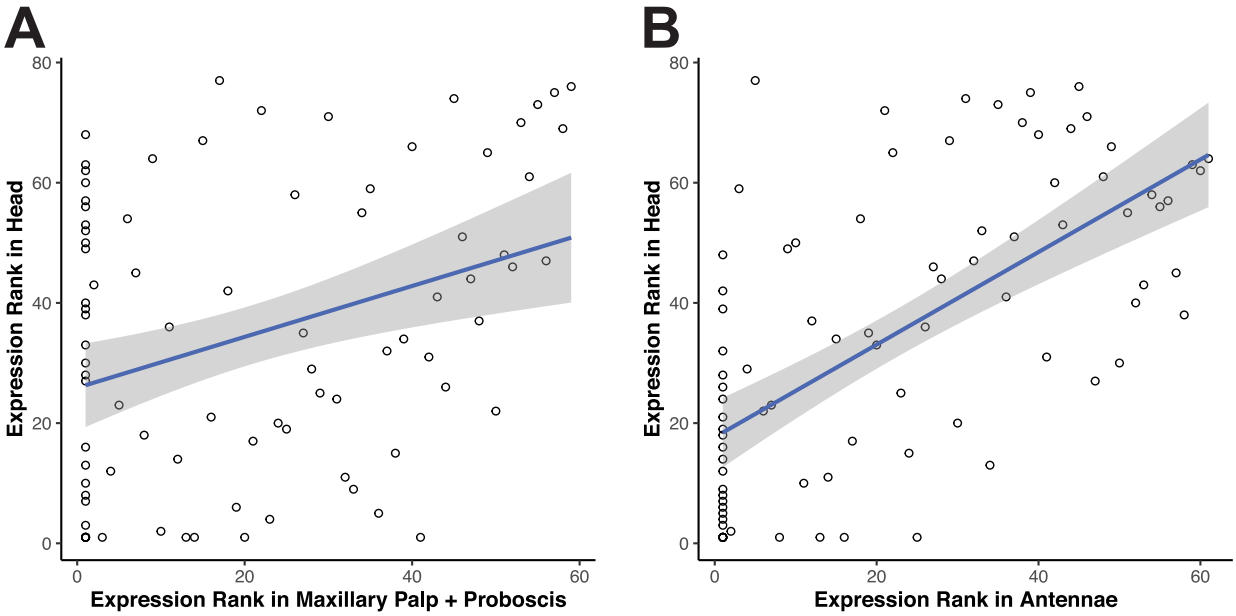

Figure S5. Correlation of expression ranking among female *D. suzukii* head and sensory organs. The relative expression for each gene in our sensory receptor gene set (Table S6) was ranked from lowest to highest in RNA-seq datasets from the maxillary palp + proboscis and antennae and compared to the ranking of expression in our head RNA-seq dataset.

Table S1. Properties of the chromosome-level assembly of the *D. subpulchrella* genome. The scaffolds listed in the table have at least 6 genes that are reciprocal best hits of *D. melanogaster* genes. Scaffold names starting with "alt_" denote alternate haplotype contigs.

***D. subpulchrella* scaffold name**	**Length (Mb)**	***D. melanogaster* chromosome homolog**	**Best hit gene number with homologous chromosome**
Seq405	29.50	3L	1985
Seq361	22.17	2R	1807
Seq355	20.23	3R	1686
Seq407	29.67	X	1572
Seq360	26.21	2L	1532
Seq354	11.59	3R	794
alt_Seq3	1.79	2L	106
Seq23	2.26	4	56
alt_Seq10	0.75	2R	46
Seq24	2.16	2R	41
alt_Seq14	0.76	2L	14
alt_Seq417	0.47	2L	11
Seq15	4.47	X	9
alt_Seq9	0.08	3R	7
Seq36	1.62	2L	6

Table S2. OR gene differential expression P-values.
OR genes that were included in the MK test were analyzed for differential expression in *D. suzukii* as compared to *D. melanogaster, D. biarmipes*, and *D. subpulchrella*, separately. P-values were calculated through pairwise *t*-tests on Log_2 transformed and normalized TPM between *D. suzukii* and the other species.

Gene Name	*D. mel - D. suz*	*D. bia - D. suz*	*D. sub - D. suz*
Or10a	0.031	0.076	0.058
Or13a	0.065	0.053	0.531
Or19b	0.282	0.632	0.662
Or1a	0.010	0.500	0.519
Or22a	0.194	0.459	0.765
Or22c	0.506	0.080	0.310
Or24a	0.272	0.939	0.913
Or2a	0.414	0.725	0.465
Or30a	0.506	0.106	1.000
Or33c	0.157	0.277	0.529
Or35a	0.136	0.283	0.220
Or42b	0.196	0.632	0.338
Or45a	0.084	0.123	0.414
Or45b	0.058	0.292	0.030
Or46a	0.069	0.155	0.335
Or47a	0.405	0.005	0.169
Or47b	0.019	0.162	0.739
Or59a	0.355	0.141	1.000
Or59c	0.876	0.022	0.016
Or63a	0.039	0.024	0.059
Or65c	0.031	0.070	0.026
Or67a	1.000	0.026	0.467
Or67b	0.087	0.060	0.060
Or67c	1.000	0.681	0.241
Or67d	0.639	0.144	0.519
Or69a	0.135	0.088	0.787
Or7a	0.543	0.792	0.385
Or85a	0.054	0.105	0.014
Or85b	0.171	0.083	0.584
Or85d	0.288	0.039	0.007
Or85e	0.843	0.092	0.053
Or85f	0.059	0.968	0.001
Or88a	0.042	0.042	0.529
Or94a	0.296	0.289	0.519
Or98a	0.351	0.028	0.029
Or98b	0.782	0.926	0.285
Or9a	0.021	0.976	0.037

Table S3. GR gene differential expression P-values.
GR genes that were included in the MK test were analyzed for differential expression in *D. suzukii* as compared to *D. melanogaster, D. biarmipes*, and *D. subpulchrella*, separately. P-values were calculated through pairwise *t*-tests on Log_2 transformed and normalized TPM between *D. suzukii* and the other species. NA – Not Applicable, gene is not expressed in either of the species in the comparison.

Gene Name	*D. mel - D. suz*	*D. bia - D. suz*	*D. sub - D. suz*
Gr10a	0.001	0.320	0.519
Gr10b	0.569	0.006	0.644
Gr21a	0.392	0.468	0.021
Gr22a	NA	0.331	NA
Gr22e	NA	0.500	0.519
Gr28b	0.073	0.504	0.787
Gr2a	0.059	0.802	0.266
Gr33a	0.092	0.675	0.520
Gr36a	0.585	0.537	0.519
Gr39a	0.369	0.019	0.834
Gr39b	0.036	0.037	0.372
Gr47b	0.007	0.002	0.003
Gr57a	NA	NA	NA
Gr58a	NA	NA	NA
Gr59a	0.506	0.395	0.519
Gr59f	0.956	0.500	0.463
Gr5a	0.784	0.234	1.000
Gr61a	0.364	0.350	0.103
Gr63a	0.103	0.858	0.000
Gr64c	0.267	0.005	0.934
Gr66a	0.003	0.000	0.004
Gr68a	0.344	0.839	1.000
Gr77a	0.009	0.000	0.354
Gr85a	0.049	0.003	0.005
Gr89a	0.124	0.500	0.275
Gr8a	0.622	0.002	0.017
Gr92a	0.074	0.057	0.424
Gr93c	0.994	0.044	0.328
Gr93d	0.924	0.113	0.909
Gr94a	0.510	0.486	0.439
Gr97a	0.006	0.013	0.000
Gr98a	0.544	0.500	0.519
Gr9a	0.506	0.611	0.028

Table S4. IR gene differential expression P-values.
IR genes that were included in the MK test were analyzed for differential expression in *D. suzukii* as compared to *D. melanogaster, D. biarmipes*, and *D. subpulchrella*, separately. P-values were calculated through pairwise *t*-tests on Log_2 transformed and normalized TPM between *D. suzukii* and the other species. NA – Not Applicable, gene is not expressed in either of the species in the comparison.

Gene Name	*D. mel - D. suz*	*D. bia - D. suz*	*D. sub - D. suz*
Ir100a	0.131	0.016	0.127
Ir11a	0.371	0.279	1.000
Ir20a	0.282	0.500	NA
Ir48b	NA	0.500	NA
Ir48c	0.824	0.360	0.200
Ir52a	0.109	0.091	0.141
Ir56c	0.946	0.338	0.519
Ir56d	0.032	0.415	0.418
Ir60e	0.116	0.016	0.029
Ir67a	NA	NA	0.334
Ir67b	0.316	0.277	0.010
Ir68b	0.273	0.976	0.489
Ir7a	0.853	0.445	0.276
Ir7b	NA	NA	0.519
Ir7c	0.142	0.902	0.670
Ir7e	NA	0.500	NA
Ir7g	0.157	0.262	0.278
Ir85a	0.652	0.001	0.532
Ir87a	0.881	0.168	0.519
Ir94e	0.172	0.046	0.519
Ir94g	NA	0.362	NA

Table S5. MR gene differential expression P-values.
MR genes that were included in the MK test were analyzed for differential expression in *D. suzukii* as compared to *D. melanogaster, D. biarmipes*, and *D. subpulchrella*, separately. P-values were calculated through pairwise *t*-tests on Log_2 transformed and normalized TPM between *D. suzukii* and the other species. NA – Not Applicable, gene is not expressed in either of the species in the comparison.

Gene Name	*D. mel - D. suz*	*D. bia - D. suz*	*D. sub - D. suz*
iav	0.008	0.002	0.060
Mid1	0.049	0.775	0.049
Nach	0.101	0.084	0.257
nan	0.239	1.000	0.857
nompC	0.068	0.149	0.112
pain	0.001	0.036	0.581
Piezo	0.077	0.005	0.149
Pkd2	0.465	0.000	0.307
ppk	0.163	0.545	0.057
ppk11	0.328	0.751	0.456
ppk12	0.932	0.200	0.576
ppk13	NA	0.043	NA
ppk15	0.084	0.003	0.350
ppk17	0.027	0.688	0.276
ppk18	0.329	0.792	0.051
ppk22	0.637	0.001	0.255
ppk23	0.506	0.013	0.083
ppk25	0.204	0.008	0.030
ppk26	0.506	0.717	0.953
ppk28	0.137	0.084	0.344
ppk29	0.866	0.053	0.150
ppk31	0.011	0.133	0.024
ppk5	1.000	0.000	0.329
ppk6	0.506	0.084	0.277
ppk8	0.591	0.946	0.195
ppk9	0.506	0.294	0.039
pyx	0.506	0.013	0.021
tmc	0.506	0.076	0.037
trpl	0.010	0.001	0.018
Trpm	0.078	1.000	0.343
Trpy	0.041	0.649	0.914
wtrw	0.145	0.001	0.001

Table S6. Sensory receptor genes used in genomic and transcriptomic analyses.
Ortholog information for OR, GR, IR, and MR genes used for the four focal species. Only genes included in the McDonald-Kreitman (MK) test are listed here. Details of MK test criteria and ortholog matching in methods.

Gene Name	*D. suzukii* Gene ID	*D. melanogaster* Gene ID	*D. biarmipes* Gene ID	*D. subpulchrella* Gene ID
Or10a	DS20_00048020	FBgn0030298	DBIA005520	augustus-dsubp_Seq407-processed-gene-75.1
Or13a	DS20_00014680	FBgn0030715	DBIA007125	maker-dsubp_Seq407-exonerate_est2genome-gene-55.12
Or19b	DS20_00111610	FBgn0062565	DBIA004964	maker-dsubp_Seq407-exonerate_protein2genome-gene-23.35
Or1a	DS20_00048650	FBgn0029521	DBIA005596	maker-dsubp_Seq407-augustus-gene-72.64
Or22a	DS20_00083610	FBgn0026398	DBIA010864	augustus-dsubp_Seq360-processed-gene-48.0
Or22c	DS20_00086700	FBgn0026396	DBIA006599	maker-dsubp_Seq360-exonerate_protein2genome-gene-58.90
Or24a	DS20_00076620	FBgn0026394	DBIA008532	maker-dsubp_Seq14-exonerate_protein2genome-gene-0.27
Or2a	DS20_00049590	FBgn0023523	DBIA005697	maker-dsubp_Seq407-exonerate_protein2genome-gene-69.65
Or30a	DS20_00092260	FBgn0032096	DBIA007003	maker-dsubp_Seq360-exonerate_protein2genome-gene-27.34
Or33c	DS20_00096670	FBgn0026390	DBIA002468	augustus-dsubp_Seq360-processed-gene-13.56
Or35a	DS20_00085320	FBgn0028946	DBIA006736	maker-dsubp_Seq360-exonerate_est2genome-gene-52.17
Or42b	DS20_00123340	FBgn0033043	DBIA015520	maker-dsubp_Seq69-exonerate_protein2genome-gene-1.0
Or45a	DS20_00129850	FBgn0033404	DBIA009648	maker-dsubp_Seq361-exonerate_protein2genome-gene-64.61
Or45b	DS20_00129670	FBgn0033422	DBIA009630	maker-dsubp_Seq361-exonerate_protein2genome-gene-65.42
Or46a	DS20_00135780	FBgn0026388	DBIA004133	maker-dsubp_Seq361-exonerate_est2genome-gene-34.8
Or47a	DS20_00137170	FBgn0026386	DBIA004259	maker-dsubp_Seq361-exonerate_est2genome-gene-37.15
Or47b	DS20_00136900	FBgn0026385	DBIA004235	maker-dsubp_Seq361-augustus-gene-37.210
Or59a	DS20_00133810	FBgn0026384	DBIA004638	augustus-dsubp_Seq361-processed-gene-54.7
Or59c	DS20_00133840	FBgn0034866	DBIA004642	maker-dsubp_Seq12-exonerate_est2genome-gene-0.2
Or63a	DS20_00003490	FBgn0035382	DBIA001054	augustus-dsubp_Seq405-processed-gene-70.12
Or65c	DS20_00005260	FBgn0041623	DBIA003777	maker-dsubp_Seq405-snap-gene-77.414
Or67a	DS20_00123090	FBgn0036009	DBIA011234	augustus-dsubp_Seq355-processed-gene-14.24
Or67b	DS20_00008700	FBgn0036019	DBIA000874	maker-dsubp_Seq405-augustus-gene-33.226
Or67c	DS20_00008100	FBgn0036078	DBIA000810	maker-dsubp_Seq405-exonerate_est2genome-gene-89.3
Or67d	DS20_00008080	FBgn0036080	DBIA000807	maker-dsubp_Seq405-exonerate_est2genome-gene-89.12

Or69a	DS20_00055820	FBgn0041622	DBIA003587	maker-dsubp_Seq405-augustus-gene-61.185
Or7a	DS20_00015570	FBgn0030016	DBIA010477	maker-dsubp_Seq407-exonerate_est2genome-gene-35.1
Or85a	DS20_00044650	FBgn0037576	DBIA001989	maker-dsubp_Seq354-augustus-gene-37.324
Or85b	DS20_00038870	FBgn0037590	DBIA002008	maker-dsubp_Seq241-exonerate_est2genome-gene-0.3
Or85d	DS20_00038820	FBgn0037594	DBIA002011	maker-dsubp_Seq354-exonerate_protein2genome-gene-37.63
Or85e	DS20_00038780	FBgn0026399	DBIA002017	maker-dsubp_Seq354-exonerate_protein2genome-gene-37.117
Or85f	DS20_00062320	FBgn0037685	DBIA002118	maker-dsubp_Seq355-exonerate_protein2genome-gene-2.25
Or88a	DS20_00053320	FBgn0038203	DBIA001455	maker-dsubp_Seq354-exonerate_protein2genome-gene-22.15
Or94a	DS20_00146650	FBgn0039033	DBIA001732	augustus-dsubp_Seq355-processed-gene-35.12
Or98a	DS20_00097740	FBgn0039551	DBIA009044	maker-dsubp_Seq355-exonerate_est2genome-gene-24.7
Or98b	DS20_00120440	FBgn0039582	DBIA005141	augustus-dsubp_Seq355-processed-gene-20.1
Or9a	DS20_00016110	FBgn0030204	DBIA007312	snap-dsubp_Seq407-processed-gene-45.136
Gr10a	DS20_00048010	FBgn0045502	DBIA005519	maker-dsubp_Seq407-exonerate_protein2genome-gene-75.11
Gr10b	DS20_00048000	FBgn0030297	DBIA005518	maker-dsubp_Seq407-exonerate_protein2genome-gene-75.10
Gr21a	DS20_00076230	FBgn0041250	DBIA008570	augustus-dsubp_Seq14-processed-gene-1.49
Gr22a	DS20_00083860	FBgn0045501	DBIA010841	augustus-dsubp_Seq360-processed-gene-47.7
Gr22e	DS20_00083850	FBgn0045497	DBIA010840	maker-dsubp_Seq360-exonerate_protein2genome-gene-46.11
Gr28b	DS20_00091740	FBgn0045495	DBIA003334	augustus-dsubp_Seq360-processed-gene-29.49
Gr2a	DS20_00050700	FBgn0265139	DBIA005880	maker-dsubp_Seq407-augustus-gene-65.148
Gr33a	DS20_00097080	FBgn0032416	DBIA002425	maker-dsubp_Seq360-exonerate_protein2genome-gene-11.52
Gr36a	DS20_00087360	FBgn0045487	DBIA003002	maker-dsubp_Seq360-exonerate_protein2genome-gene-59.7
Gr39a	DS20_00089860	FBgn0264556	DBIA002732	augustus-dsubp_Seq360-processed-gene-36.9
Gr39b	DS20_00089920	FBgn0041245	DBIA002724	snap-dsubp_Seq360-processed-gene-35.21
Gr47b	DS20_00136850	FBgn0041241	DBIA004230	maker-dsubp_Seq361-exonerate_protein2genome-gene-36.86
Gr57a	DS20_00136720	FBgn0041240	DBIA004215	maker-dsubp_Seq361-exonerate_protein2genome-gene-36.33
Gr58a	DS20_00128240	FBgn0041239	DBIA004802	maker-dsubp_Seq361-snap-gene-69.168
Gr59a	DS20_00129160	FBgn0045483	DBIA004706	maker-dsubp_Seq361-exonerate_protein2genome-gene-67.12
Gr59f	DS20_00133950	FBgn0041234	DBIA004654	maker-dsubp_Seq361-exonerate_protein2genome-gene-54.22
Gr5a	DS20_00102140	FBgn0003747	DBIA011874	augustus-dsubp_Seq407-processed-gene-97.20

Gr61a	DS20_00001190	FBgn0035167	DBIA010640	maker-dsubp_Seq405-exonerate_est2genome-gene-51.9
Gr63a	DS20_00074380	FBgn0035468	DBIA000047	maker-dsubp_Seq405-augustus-gene-35.103
Gr64c	DS20_00053760	FBgn0045477	DBIA000072	maker-dsubp_Seq405-snap-gene-36.291
Gr66a	DS20_00010480	FBgn0035870	DBIA001123	maker-dsubp_Seq405-exonerate_protein2genome-gene-97.147
Gr68a	DS20_00071190	FBgn0041231	DBIA012033	maker-dsubp_Seq405-exonerate_protein2genome-gene-27.61
Gr77a	DS20_00003900	FBgn0045474	DBIA003934	maker-dsubp_Seq405-exonerate_protein2genome-gene-72.54
Gr85a	DS20_00038310	FBgn0045473	DBIA001538	maker-dsubp_Seq354-exonerate_protein2genome-gene-32.49
Gr89a	DS20_00065090	FBgn0038440	DBIA011120	maker-dsubp_Seq355-augustus-gene-11.147
Gr8a	DS20_00105100	FBgn0030108	DBIA006013	maker-dsubp_Seq407-snap-gene-84.248
Gr92a	DS20_00019880	FBgn0045471	DBIA001362	maker-dsubp_Seq354-exonerate_protein2genome-gene-18.12
Gr93c	DS20_00000030	FBgn0045469	DBIA001929	augustus-dsubp_Seq0-processed-gene-0.11
Gr93d	DS20_00000040	FBgn0045468	DBIA001928	maker-dsubp_Seq0-snap-gene-0.81
Gr94a	DS20_00025130	FBgn0041225	DBIA001723	maker-dsubp_Seq355-protein2genome-gene-35.105
Gr97a	DS20_00041320	FBgn0041224	DBIA007734	maker-dsubp_Seq355-exonerate_protein2genome-gene-55.32
Gr98a	DS20_00097520	FBgn0039520	DBIA005065	maker-dsubp_Seq355-exonerate_protein2genome-gene-23.13
Gr9a	DS20_00104450	FBgn0052693	DBIA011665	augustus-dsubp_Seq407-processed-gene-90.1
Ir100a	DS20_00068470	FBgn0039879	DBIA014431	maker-dsubp_Seq355-protein2genome-gene-66.170
Ir11a	DS20_00111940	FBgn0030385	DBIA005011	maker-dsubp_Seq407-exonerate_protein2genome-gene-24.22
Ir20a	DS20_00120950	FBgn0031181	DBIA012954	augustus-dsubp_Seq407-processed-gene-13.282
Ir48b	DS20_00139560	FBgn0033648	DBIA006097	maker-dsubp_Seq361-exonerate_protein2genome-gene-44.33
Ir48c	DS20_00139610	FBgn0033651	DBIA006102	maker-dsubp_Seq361-exonerate_protein2genome-gene-44.34
Ir52a	DS20_00034570	FBgn0034023	DBIA006570	snap-dsubp_Seq361-processed-gene-20.51
Ir56c	DS20_00143920	FBgn0034457	DBIA010251	maker-dsubp_Seq361-exonerate_protein2genome-gene-51.56
Ir56d	DS20_00143930	FBgn0034458	DBIA010253	maker-dsubp_Seq361-exonerate_protein2genome-gene-51.32
Ir60e	DS20_00133340	FBgn0035019	DBIA004598	maker-dsubp_Seq361-exonerate_protein2genome-gene-55.71
Ir67a	DS20_00008790	FBgn0036010	DBIA000885	maker-dsubp_Seq405-exonerate_protein2genome-gene-32.130
Ir67b	DS20_00008060	FBgn0036083	DBIA000802	maker-dsubp_Seq405-exonerate_protein2genome-gene-88.26
Ir68b	DS20_00005790	FBgn0036250	DBIA000546	maker-dsubp_Seq405-exonerate_protein2genome-gene-78.39
Ir7a	DS20_00029670	FBgn0029961	DBIA013727	maker-dsubp_Seq407-exonerate_protein2genome-gene-37.13

Ir7b	DS20_00029730	FBgn0029965	DBIA015424	maker-dsubp_Seq407-exonerate_protein2genome-gene-36.42
Ir7c	DS20_00029750	FBgn0029966	DBIA015422	maker-dsubp_Seq407-exonerate_est2genome-gene-36.10
Ir7e	DS20_00029770	FBgn0259189	DBIA015421	maker-dsubp_Seq407-exonerate_protein2genome-gene-36.43
Ir7g	DS20_00029780	FBgn0029968	DBIA015420	maker-dsubp_Seq407-exonerate_protein2genome-gene-36.58
Ir85a	DS20_00039730	FBgn0037630	DBIA002046	augustus-dsubp_Seq355-processed-gene-0.17
Ir87a	DS20_00150770	FBgn0038153	DBIA001378	maker-dsubp_Seq354-exonerate_protein2genome-gene-18.11
Ir94e	DS20_00123140	FBgn0259194	DBIA005346	augustus-dsubp_Seq355-processed-gene-47.16
Ir94g	DS20_00123170	FBgn0039079	DBIA005349	augustus-dsubp_Seq355-processed-gene-47.17
iav	DS20_00049250	FBgn0086693	DBIA005662	maker-dsubp_Seq407-exonerate_est2genome-gene-70.0
Mid1	DS20_00133010	FBgn0053988	DBIA004559	maker-dsubp_Seq361-exonerate_protein2genome-gene-56.37
Nach	DS20_00130410	FBgn0024319	DBIA009703	maker-dsubp_Seq361-snap-gene-63.184
nan	DS20_00006980	FBgn0036414	DBIA000672	maker-dsubp_Seq405-exonerate_est2genome-gene-83.0
nompC	DS20_00077950	FBgn0016920	DBIA008361	maker-dsubp_Seq360-exonerate_est2genome-gene-76.2
pain	DS20_00127130	FBgn0060296	DBIA004909	augustus-dsubp_Seq361-processed-gene-72.64
Piezo	DS20_00093040	FBgn0264953	DBIA006910	augustus-dsubp_Seq360-processed-gene-22.7
Pkd2	DS20_00097250	FBgn0041195	DBIA002408	augustus-dsubp_Seq360-processed-gene-13.18
ppk	DS20_00084990	FBgn0020258	DBIA006781	maker-dsubp_Seq360-exonerate_est2genome-gene-50.9
ppk11	DS20_00092900	FBgn0065109	DBIA006927	maker-dsubp_Seq360-exonerate_protein2genome-gene-22.40
ppk12	DS20_00143270	FBgn0034730	DBIA010186	maker-dsubp_Seq361-exonerate_est2genome-gene-29.6
ppk13	DS20_00086820	FBgn0053508	DBIA003055	maker-dsubp_Seq360-exonerate_protein2genome-gene-58.87
ppk15	DS20_00101720	FBgn0039424	DBIA007678	maker-dsubp_Seq355-exonerate_protein2genome-gene-57.9
ppk17	DS20_00080850	FBgn0032602	DBIA012741	maker-dsubp_Seq360-exonerate_protein2genome-gene-36.85
ppk18	DS20_00092860	FBgn0265001	DBIA006928	maker-dsubp_Seq360-snap-gene-22.88
ppk22	DS20_00012680	FBgn0051105	DBIA001671	maker-dsubp_Seq355-snap-gene-64.219
ppk23	DS20_00051210	FBgn0030844	DBIA005824	maker-dsubp_Seq407-exonerate_est2genome-gene-63.11
ppk25	DS20_00033500	FBgn0053349	DBIA006456	maker-dsubp_Seq361-snap-gene-17.700
ppk26	DS20_00109310	FBgn0035785	DBIA004070	maker-dsubp_Seq405-exonerate_protein2genome-gene-41.29
ppk28	DS20_00113000	FBgn0030795	DBIA010422	maker-dsubp_Seq407-exonerate_protein2genome-gene-53.9
ppk29	DS20_00141090	FBgn0034965	DBIA009945	maker-dsubp_Seq361-snap-gene-22.145

ppk31	DS20_00074820	FBgn0051065	DBIA007762	augustus-dsubp_Seq355-processed-gene-54.31
ppk5	DS20_00149700	FBgn0053289	DBIA011492	maker-dsubp_Seq405-exonerate_protein2genome-gene-17.40
ppk6	DS20_00035060	FBgn0034489	DBIA008216	augustus-dsubp_Seq361-processed-gene-48.26
ppk8	DS20_00017250	FBgn0052792	DBIA007172	maker-dsubp_Seq407-exonerate_protein2genome-gene-50.14
ppk9	DS20_00128290	FBgn0085398	DBIA004798	maker-dsubp_Seq361-augustus-gene-69.140
pyx	DS20_00000480	FBgn0035113	DBIA010564	maker-dsubp_Seq405-exonerate_protein2genome-gene-54.43
tmc	DS20_00008720	FBgn0267796	DBIA000876	maker-dsubp_Seq405-snap-gene-33.237
trp1	DS20_00129450	FBgn0005614	DBIA009598	maker-dsubp_Seq361-exonerate_est2genome-gene-66.2
Trpm	DS20_00034790	FBgn0265194	DBIA009896	maker-dsubp_Seq361-exonerate_est2genome-gene-21.0
Trpy	DS20_00080660	FBgn0032593	DBIA012719	maker-dsubp_Seq360-exonerate_est2genome-gene-36.7
wtrw	DS20_00119270	FBgn0260005	DBIA008758	augustus-dsubp_Seq354-processed-gene-6.71

Table S7. Sensory receptor expression patterns in abdominal tip.
The expression (in Transcript Per Millions) of OR, GR, IR, and MR genes in the abdominal tip RNA-seq data for the genes that were under selection in the MK test in at least one species. Expressed genes are listed first. The most highly expressed sensory genes in the abdominal tip tissue are mechanosensory receptors. Most of OR, Gr and IR genes show little or no expression in the abdominal tip. TPMs are raw values for each species and are not normalized for samples between species. Expressed denotes genes showing TPM larger than 1 in at least one of the four species.

Gene Name	*D. suzukii*	*D. subpulchrella*	*D. biarmipes*	*D. melanogaster*	Expressed
Or47a	0.081	0.434	1.336	0.515	Yes
Or85f	0.062	23.286	3.624	0.599	Yes
Gr39a	0.196	0	1.152	1.012	Yes
Gr63a	1.978	7.836	0.429	0.112	Yes
Gr64c	0	0	5.273	0.057	Yes
Ir87a	1.086	0.151	0.058	0.155	Yes
iav	1.079	1.573	13.307	0.572	Yes
Ir87a	1.086	0.151	0.058	0.155	Yes
nan	0.029	0	1.457	0.252	Yes
nompC	0.705	0.569	0.678	1.3	Yes
Piezo	25.339	20.195	8.238	15.818	Yes
Pkd2	0.152	0.476	16.248	0.042	Yes
ppk	1.976	2.278	4.353	2.365	Yes
ppk13	0.052	0	6.399	0.151	Yes
ppk17	13.025	21.831	12.007	0.957	Yes
ppk22	0.152	0	19.193	0.082	Yes
ppk26	2.987	4.15	4.452	2.313	Yes
tmc	0.158	0.114	1.287	1.108	Yes
trp1	0.535	1.069	0.234	0.699	Yes
trpm	5.756	5.836	11.108	8.171	Yes
wtrw	19.143	21.61	26.798	9.313	Yes
Or10a	0.082	0.091	0.122	0	No
Or13a	0.107	0	0.556	0	No
Or19b	0.024	0.328	0.037	0	No
Or1a	0	0	0	0.485	No
Or22a	0.027	0	0.145	0.259	No
Or2a	0.526	0.57	0.31	0	No
Or30a	0	0	0	0	No
Or33c	0.097	0	0	0	No
Or35a	0	0.07	0	0	No
Or45a	0	0	0.155	0.013	No
Or45b	0	0	0.101	0	No

Or46a	0	0.163	0.11	0	No
Or47b	0	0	0	0.04	No
Or63a	0	0	0	0.027	No
Or65c	0	0	0	0.413	No
Or67a	0	0	0	0.033	No
Or67b	0.149	0	0.4	0	No
Or67c	0	0	0	0.04	No
Or67d	0	0.158	0	0	No
Or69a	0	0	0	0	No
Or7a	0	0.224	0.129	0.29	No
Or85a	0	0.525	0.385	0	No
Or85b	0	0	0.039	0	No
Or85d	0	0	0.097	0	No
Or85e	0	0	0	0.042	No
Or88a	0	0	0	0	No
Or94a	0	0.119	0.172	0.15	No
Or98b	0	0	0	0	No
Or9a	0	0.255	0	0.076	No
Gr10a	0	0	0	0.179	No
Gr10b	0	0	0.313	0.129	No
Gr21a	0.045	0	0.045	0.2	No
Gr28b	0.365	0.329	0.16	0.546	No
Gr2a	0.275	0.279	0	0.079	No
Gr33a	0.132	0	0	0.18	No
Gr36a	0	0	0.036	0	No
Gr39b	0.359	0.715	0	0.03	No
Gr57a	0	0	0	0	No
Gr5a	0.067	0.135	0.246	0.089	No
Gr61a	0.065	0.1	0	0.131	No
Gr68a	0	0	0	0.113	No
Gr77a	0.135	0.627	0	0.404	No
Gr89a	0	0	0.08	0.137	No
Gr93c	0	0	0.188	0	No
Gr93d	0	0	0.354	0.051	No
Ir11a	0	0	0.032	0	No
Ir48b	0	0.046	0.032	0.064	No
Ir56c	0	0	0.53	0	No
Ir56d	0.052	0	0	0	No
Ir67a	0	0	0	0.057	No
Ir67b	0	0.08	0.018	0	No

Ir68b	0.073	0.066	0.235	0.061	No
Ir7a	0	0	0	0	No
Ir7c	0.051	0.065	0.113	0.12	No
Ir7e	0	0	0.022	0	No
Ir94e	0	0	0.063	0.058	No
Nach	0.229	0	0.066	0.073	No
pain	0.082	0.029	0.584	0.454	No
ppk12	0	0.122	0.106	0.147	No
ppk15	0	0	0.057	0.023	No
ppk23	0	0.141	0.275	0.324	No
ppk25	0.022	0	0.048	0.067	No
ppk29	0.188	0.078	0.128	0.333	No
ppk6	0	0	0.23	0.201	No
ppk8	0.043	0	0.633	0.032	No
ppk9	0.027	0	0	0.042	No
Trpy	0.082	0.029	0.584	0.454	No